Detailed Response to the Reviewers

Ms. Ref. No.: esurf-2019-46

Title: A new method for calibrating marine biota living-depth using the 2016 Kaikōura Earthquake uplift

Dear Editor,

On behalf of my co-authors, I am now in the pleasant position to return to you the revised version of our manuscript, together with the detailed answers to all the comments raised by the reviewers of this manuscript.

Overall, the comments of the two reviewers were positive and helped improve the manuscript.

You will find that we have responded to each of the general reviewers' comments and have substantially changed the manuscript accordingly. In particular, the text of the Methodology section has been changed to make it more readable and improve clarity. In line with improving this section, we have modified the title, which we feel now more accurately reflects the purpose of the paper. We have accepted and included most of the specific comments. Please, accept where we can provide a clear reason not to. We have also modified Figures 3 and 5 to accommodate the reviewers' comments while retaining lack of clutter.

In summary, we do hope that this revised version, together with our detailed response to the numerous review comments, will convince you that our work warrants publication in the Journal of Earth Surface Dynamics.

In the following paragraphs, we carefully address the comments and suggestions of:

- *Brendan Duffy (Reviewer 1) and*
- *the Anonymous Reviewer ≠2*

Our responses appear in 'red italics' while the comments of the Reviewers appear in black.

Yours sincerely

Vasiliki Mouslopoulou

Response to the comments of Brendan Duffy

Dear Editor,

Re: Reid et al. : A new method for calibrating marine biota living-depth using the 2016 Kaikōura Earthquake uplift

Thank you for the opportunity to comment on this manuscript. The authors have developed a

method of using tide tables and ecological understanding of tidal biozones to determine coseismic surface uplift from the elevation of stranded algal anchors. They present these results alongside biological estimates underpinned by a tide gauge calibration, and compare the results of all with the vertical component of differential lidar and locally a strong motion sensor. Their short discussion summarizes the results and discusses the systematic deviation from the Lidar measurements.

The method is novel and but the paper unfortunately lacks punch in the discussion, which goes nowhere really. The first two paragraphs are basically a summary and the third paragraph discussion of systematic deviation from Lidar measurements of uplift (figure 5b) and what they mean for the calibration is limited to invoking fluctuations. If the fluctuations are on the order of minutes, and the tide level was measured repeatedly at a site, can the consistent high estimates be put down to fluctuations? At line 427 (While the influence…) they say that fluctuations in the tide are mitigated by using tide gauge, but surely the estimates there were obtained using the various correction factors and local sea level measurements. My reading is that the tide gauge was only used to establish the correction, and not thereafter.

Intuitively, one would expect the RTK-tide gauge correction to be the most robust. That is borne out by the RTK-tide gauge correction around the tide gauge, which was within plus/minus 7 cm of correct while tide table corrected results varied more widely. At other sites (e.g. Paia point) each group of individual assessments are within 5% of each other but there can be 20% discrepancy from one group to the next, and with respect to the Lidar estimate. It seems to me as though the correction is reasonably precise (suggesting that the underlying concept is robust) but also quite inaccurate.

If I was a coastal ecologist I would be interested in that. Obviously local wave climate or tidal fluctuations can be a factor, as they discuss, but it may also be more interesting than that. The X-factor is a positive elevation value and is subtracted, so if the uplift is too high (most places), then not enough has been subtracted and the organism is actually shallower dwelling relative to MLWS. If the uplift value is too low, then too much has been subtracted and the organism is deeper dwelling relative to MLWS (Kaikoura harbour). Both the tide gauge and the harbour are presumably very sheltered and also areas of boat traffic, which must have some impact on marine algae distribution. The only site that yielded a too-low estimate was Kaikoura Harbour, where boat traffic and maybe sheltering is greatest. Given that in most cases the correction is too small, it may be that the organisms actually range further above MLWS than expected, while still remaining below MLWN. At Paia Point, it seems that the algae attached to rocks furthest to seaward are the most undercorrected, suggesting that those rocks (in an area where they will be bathed regularly by swell and wave action, even at the lowest tides) have the shallowest depth range.

Response *– yes, wave action is a factor in the distribution of inter-tidal species. The higher the wave exposure the higher the wave splash and, therefore, the higher the extent of species. However species respond over a seasonal or average annual cycle, and thus at the time of visiting it may be impossible for the geologist viewer to measure this effect, and it is inherent as potential error in our methodology. As described by the reviewer this effect has become apparent in a semi-measurable capacity in this study, but these measurements are specific to this part of the coast (so thus may be of interest to local ecologists) but globally are almost meaningless. The error is accommodated statistically in this study, by dealing with average elevation of upper limits of each species' holdfasts. Variation in aspect and wave exposure are site specific and have been accommodated within the statistics of captured data. No pre-earthquake measured data is available by site, and even if it was, the granularity of the bouldery intertidal environment means that changes in these factors are likely to have been wrought by coseismic uplift.*

Another thing that would be informative is to know what timescale this technique is available over. The authors carried out their work after a few months, but how much longer could they have realistically applied the technique. Also, is the 20 holdfasts that seems to be their lower limit statistically valid. If the authors take their first five, ten, twenty measurements at a site, does the result change significantly. Would it improve if they used fifty? Maybe start by showing the number of measurements of each type on Figure 5. Maybe somehow on Figure 6 too.

Response – *The timescale of organic decay following coseismic uplift would vary by location, time of year, and organism targeted. Also, d*ecay of the holdfasts and remaining algal fronds was variable with aspect. In dry, sunny places, for example, the holdfasts measured were highly decayed and rudimentary, while in some places algal fronds were still present, even at the same site. *Additional comments are made at lines 459-461 to incorporate the reviewer's feedback. Figure 5 adjusted to include "n" number of measurements, as a comparison to the data ranges already given. This is not done for other figures, as the figures become so cluttered as to be unreadable. Further, besides for each data point presented in Figure 5, we have now included in the figure the mean value.*

One strategy for the discussion is already present in the introduction. The authors provide an extensive list of coastal uplifts and biological assessments thereof in the introduction. I have always thought that the discussion should revisit the key points of the introduction. So, please revisit that list and discuss the advantages and limitations of this technique. How many historic earthquakes have caused coastal uplift, what magnitudes of coastal uplift have been documented, using what biological indicators. Which of them could have been targeted with this technique, and over what timescale. Maybe put together a useful chart/table showing the preservation potential, accuracy, precision, ease of deployment, best vertical resolution (critical if you want to document uplifts of half a meter or less), speed of survey, skill requirements, etc of the various techniques and illustrating why this one is important – I am thinking something like Table 2B in Quigley et al. (2016), in which the lead author was responsible for another biological assessment of vertical displacement. Or maybe a McCalpin style graphic. Whatever you do, please re-read your introduction and use it to put some spice into the discussion.

Response – *This paper is presenting a new methodology, and does not seek to be a review paper, which is what is implied here. While a review that compared all methodologies for past earthquakes may be useful, it is also incredibly difficult, for these or any authors to provide realistic commentary that the reviewer is requesting. Ultimately preservation potential, vertical resolution, precision and biological indicator used are all local effects, and should be determined by local or location informed reviewers (as was the case with the lead authors role in Quigley et al 2016).*

These are just a few ideas, but I really think the author team is uniquely qualified to lead this discussion towards a useful earthquake-ecology viewpoint, especially given the lead author's established expertise in biological zonation (Reid et al., 2011 - their fig 2 deserves a citation here) and earthquake effects on that in New Zealand (Quigley et al., 2016). One way or another the discussion needs to be beefed up. A brief discussion of some of these points, possibly using these results to think further about some previous Reid et al work, would probably find favour with coastal ecologists and increase the citability of the paper. A table or graphic of the kind I suggest above would surely contribute to the quantitative coastal ecological impact assessments that will follow future earthquakes, in New Zealand and elsewhere.

Enough long-winded discussion of the discussion (eek). Another key criticism relates to the description of the methods. I found this opaque, with many ambiguities. The opacity is largely because the paper dives straight into formulae without really explaining the strategy. This is not helped by a major discrepancy between the formula shown in text and that shown in Figure 3.

After some careful checking I am happy that the methods are valid but they need to be clarified and subscripts used consistently. I also see little indication of the uncertainties in the figures. They are covered to a certain extent in the text, but there are no error bars on major figures (e.g. Fig 6).

Response *– the more detailed comments of the reviewer, that certainly improve the clarity of the methodology, have all been addressed below. Error bars are not included on some figures (e.g. Fig 6) as this would result in cluttering and unnecessary complication of those figures. However, all data, together with their uncertainties, are presented in the tables that accompany this manuscript.*

Below I provide detailed comments and corrections, mostly regarding the methods and description thereof. There may be some errors of understanding on my part and I apologise for any such errors contained here.

Once again, thank you for this opportunity and good luck to the authors. I look forward to seeing this published.

Sincerely,
Brendan

Detailed comments

Line 25: Satellite data is ubiquitous, Lidar replacement is the real target here.
Response: *Sentence updated.*

Line 31: Surely Darwin could get a mention here?
Response: *This is already present in more detail at lines 56-59. Graham (1824) was the initial user of this technique, rather than Darwin, and the reference to the Beagle voyage is present in Fitzroy (1839).*

Line 78: Not convinced this is the right reference. What about Williams et al. (2013)?
Response: *Eberhart-Phillips & Bannister 2010 comprehensively map the seismicity and Vp/Vs variations in 3 dimensions within the upper plate and slab in the Marlborough region.*

Line 83: An earthquake network comprises several faults. An earthquake is a process that ruptures a fault or a network of faults. An earthquake does not comprise a network of faults.
Response: *Sentence revised at lines 116 and 117.*

Line 97: Vaguely and unintentionally implies that the mapped surface faults and coastal uplift, as well as the tsunami, extended 250 km south of Kaikoura.
Response: *Punctuation corrected at line 141 to remove this implication. Sentence modified, as well.*

Line 102: Here and elsewhere (e.g., line 103, 105, 114…), the word 'exposed' and derivatives of that word are used in two different senses of the word – Exposed coastlines and exposed holdfasts. Sometimes it is clear from context and sometimes it requires a double read to figure it out. Please consider using expos… in one sense only and replacing the other meaning with a different word. Line

114 is particularly bad – controlled by exposure above the tide? Lack of shelter? It is not an easy issue to address but maybe keep exposed for 'unsheltered' and use qualifications such as subaerially-exposed, terrestrially-exposed, outcropping, etc for stuff that is above sea level.
Response: *The text is revised at lines 146, 148, 150-151, 155, 158, 163, 187, 197, 199 and 201. This was an issue that had been addressed, but the comments of an external reader are appreciated in continuing to improve this issue. "exposed" is common terminology to describe coasts impacted by ocean swell and waves, and likewise "exposed" is used by geologists to refer to rocks in outcrop. In this manuscript exposed is retained and clarified for use with reference to coasts, and modifications or synonyms are used in geological contexts.*

Line 106: It is not diurnal, it is semi-diurnal, with two full cycles daily.
Response: *Corrected at line 151.*

Line 188: It seems to me that you never explicitly state the tide gauge uplift except in Table 1. Why not?
Response: *The results of calculations to determine uplift using the tide gauge are given in the results section. This is not included in this methods section.*

Line 189: Change to "Biological data collection" and then add a new section title at line 220 - "Data processing"
Response: *Change made and new heading added, and section 3 subheading numbering updated*

Line 211: Were the wave effects given a plus-minus value?

Response: *No. The wave effects are intrinsically variable across minutes, hours, days and seasons, and the goal was to measure water-level and the height of holdfasts above water-level. The text has not been adjusted here, as to do so adds an unnecessary complication.*

Line 213: Was sea-level re-measured after each group of twenty?
Response: *Yes. The text has been updated at line 306-307 to clarify this.*

Lines 215-218: As somebody with building experience I would have forgotten about the tape and used either 1) a builder's laser level and a reflective staff. Measure the height of the laser level mount with a tape, then measure the height of holdfasts in all positions using a reflective staff. Laser levels are small, portable, and cheap as chips and the staff could be a stick with a high vis jacket. Any holdfast accessible with RTK could be done with a laser level, especially in the late evening, and would yield similar accuracy to RTK. 2) Even cheaper, a homemade water level, with the reservoir placed on a local high point. Engineers used commercial versions widely after the Chch earthquake to survey floor levels. (https://en.wikipedia.org/wiki/Water_level_(device))
Response: *We appreciate the value of laser levels, but their use during bright day-light hours is problematic; the best time for biological data collection was during mid- to low- tides commonly during high lighting conditions. The homemade level suggestion is indeed a very cheap and simple method to get data that may have been more accurate that our tape measure method, and I am sure readers of this review will appreciate it! Our goal at the time of collection was to go with a simple low-tech method with equipment that most people would already have in their possession.*

No changes to text made.

Line 220: New section title here - maybe "3.3 Data Processing".
Response: *Done*

Line 221: These field measurements of apparent uplift… [No. they are field measurements of exposure above a reference tide level. Nobody would consider that to be apparent uplift because it is a time-dependent measurement] were then further processed to determine the total uplift [No. uplift is either of rock or surface – in this case both are equivalent at this moment in time, so just say surface uplift], taking into account the time of data measurement and the pre-earthquake living position of the algal holdfasts which is the difference between pre- and post-earthquake elevation of algal holdfasts [Note that position is a 3D thing and we are only interested in z, not x or y].
Response: *The text is modified at lines 317-318.*

Line 222: Just say "Three different corrections were used to derive surface uplift from elevation above sea level at a point in time. These were a) tide gauge calibration; b) interpolation of NIWA tide forecaster and c) interpolation of LINZ tide forecaster. Method a) calculated a correction using direct measurement of stranded algae relative to the
Response: *On reviewing this section of text and the reviewers recommendations we feel changing the text as recommended would add further confusion. The correction factor (our terminology) was derived in slightly different ways, but it was only one part of the overall calculation of uplift. Uplift is known at the Kaikoura tide gauge, whereas methods b) and c) combined the tide forecaster interpolation with local knowledge of biological living zones. Although more subjective, corrections b and c are applicable to sites where no tide gauge is available.*

Line 229: A factor is a number that is multiplied by another to yield a product. This is not a factor, it is a constant. There is also more than one constant.
Response*: In a general sense, as is often applied in science text, this is meant as an adjustment to an equation to account for a known variation. However, in a pure mathematical sense, the reviewer's definition of factor is correct. As there is more than one constant in this study, and this value would need to be re-calculated at any other location we are not comfortable defining this as a correction constant – the term constant implies our correction value could be applied globally. It cannot, but the calculation can be. On this basis, we have revised the text to use the term 'correction' throughout.*

Line 229: I suggest that you change title to "Correction a) Deriving living depth constants for target species using the Kaikoura tide gauge."
Response*: It is not clear how this would improve the heading …..*

Lines 230-250: Try and be a little kinder to those who want to reproduce this. I found it very hard to follow until I figured out what you were doing. Maybe describe in words what you are doing, rather than diving straight into the derivation of your constant. I recommend: "Surface uplift is the difference between the present, post-uplift elevation and the pre-uplift elevation (the living elevation) of the organisms holdfasts. The target species occupy slightly different living positions in the inter-tidal zone, so this new method first derives a constant living elevation (X, in m) for each target species (XC – Carpophyllum; XD – Durvillaea; Combined XG), by calculating the pre-

earthquake elevation of the stranded holdfasts relative to the spring-tide mean low water level (MLWS). The constant XC/D/G is calculated in three stages, using holdfasts at sheltered sites close to the Kaikoura tide gauge. First the height of the stranded holdfast above the uplifted tide gauge mount is calculated from the sum of the tide gauge height and the observed elevation of the stranded holdfast relative to sea level (both at measurement time). Secondly, the tide gauge uplift is subtracted obtain the elevation relative to the pre-quake tide gauge. Finally, MLWS is further subtracted to obtain elevation relative to MLWS, which is a key reference level for the biological zonation.
This procedure is given by the equation: ... where
Response*: The text has been modified starting at line 327 to improve clarity. The text is kept at the calculation of the correction, rather than including reference to surface uplift as suggested by the reviewer, as this seemed to remove the focus from the immediate topic. We are grateful to the reviewer for this suggestion, and the time taken to suggest suitable text for an external audience.*

Line 231: Depth implies below sea level. At least one species lived above MLWS, so depth would be negative. Just use elevation, since you are differencing with elevation.
Response*: Living-depth was used in reference to the tidal cycle of MLWS to mean high water spring. However as we calculate the living "depth" with respect to MLWS, this is changed to living position throughout the manuscript.*

Line 235: Bit of a mess here. Outer parentheses are redundant. The MLWS subtraction is not shown in the equation on Figure 3. Figure 3 uses HTG instead of H, so please be consistent.
Response*: Equation in text tidied up, and MLWS re-inserted into Figure 3. Subscripts are checked and corrected throughout the manuscript.*

Line 240: subscripts rather than indices?
Response*: corrected*

Line 241: … average post-uplift tide gauge reading…
Response*: Adjusted*

Line 244: You have already said they occupy different levels, especially if you adopt the text above, so just leave out the first sentence of this paragraph.
Response*: The first sentence is retained, as this text is intended to clarify the use of C/D/G with respect to X, and why these need to exist. The text suggestion for line 230 was not adopted verbatim.*

Line 247: "Further, only …." – This should appear within the derivation of the formula. See comment for line 230 above.
Response*: Adjusted*

Line 256: You introduce a parameter without defining it (UB(TG)). Sure I can work out what it is but I shouldn't need to. Also H in eqn 2 looks a lot like H in eqn 1. Hence the need to use HTG in eqn 1. Each time you use H it refers to a specific time and place. I wonder if you need to have HTG and HSS (survey site). One way or another your subscripts need to be unique, informative and consistent,

because at the moment they are not. I recommend that you include a glossary of the terms used in your equations.
Response: *UB(TG) is defined. H is indeed HTG and this is adjusted.*

Line 265: Please clarify this process. Maybe change text beginning line 265 to read... "where OMCDG is the observed elevation of the holdfasts relative to locally measured sea level, HNIWA/LINZ is the difference between the predicted tide height at survey time and the MLWS based on one year of predictive tables, and XC/D relies on expert assessment as follows: Carpophyllum..." Note here, please be consistent with subscripts. I cant see any reason why OM here would be different to OMC/D/G in equation 1. Also, how would you get an expert assessment of tidal zonation in Timor for instance?
Response: *Text is adjusted, although not quite as recommended above (HNiwa is not linked to MLWS as written above). Subscripts have been reviewed and adjusted throughout. Working in other locations would require talking to local marine biologists, or local fisherman to understand their observations of local conditions.*

Line 272: What is a regional height?
Response: *Sentence adjusted for clarity. Refers to Kaikōura region.*

Line 274: Replace height with holdfast elevation (height is a vague term)
Response: *Change made*

Line 285: Why are NIWA and LINZ different? Can you illustrate the difference in a figure, or summarize it somehow?
Response: *Text is adjusted at lines 428-429 to accommodate this. The LINZ charts provide data for fixed geographical locations. The NIWA forecaster uses a model to predict tidal height at any geographical point, between the LINZ fixed points.*

Line 292: The absolute accuracy of RTK may be 5 cm vertical if you put your base station on a suitable order trig. The internal relative accuracy is better than that (2 cm) with favourable GPS environment (see e.g table 1 in Duffy et al. 2013). On that note, where was your base station set up? Maybe it doesn't matter, if all of your RTK measurements were differenced with a local sea level measurement every 10 minutes or so but you should still mention it. Personally, I would have opened and closed the survey at the tide gauge, so that I could see how well my sea level measurements replicated the tide gauge.
Response: *A base station was not used in this case, as the internal accuracy of the difference between holdfast elevation and waterline elevation was the key data required. Absolute measurements were not taken, and would have required the more time consuming use of a base station and calibration. A minor change made in the methods section to clarify no base station was used.*

Line 314: Please check figure order. I haven't checked super carefully, but Fig 7 seems to come before 5 and 6. Please make sure they are numbered in order.
Response: *Reference to figure 7 at line 330 is removed, and reference to Fig. 7 is only made in the results section, as it displays results.*

Line 320: The problem with the lidar at Kaikoura harbour should be mentioned here, not in the results. And really, I want to know how inconsistent they were. If you do a histogram over a couple of roads around the harbour, what do you get? Is it consistent with the strong motion instrument or not?

Response*: Thanks to the reviewer for asking this question. In answer, differential LiDAR data was not available immediately adjacent to the Kaikōura Harbour site. Extrapolation from other regions produced variable results, with none able to be realistically used, or any source able to be justified over another. The text is modified at line 482 and line 576.*

Line 336: New heading - 4.1 Tide gauge locality

Response*: New heading inserted at line 506*

Line 339: Delete sentence - "Uplift estimates derived…"

Response*: Sentence deleted.*

Line 344: … tide gauge (Figure 5) and compared with uplift of the Kaikoura tide gauge (calculated in section 3.1)

Response*: Text adjusted.*

Line 370: New section title here - maybe "4.2 Paia Point and Omihi Point".

Response*: New heading inserted at line 552.*

Line 392: How inconsistent? And why? Differential beach gravel compaction? Something else? Does this inconsistentcy affect have any effect over the distance from strong motion sensor to measurement sites?

Response*: This is resolved by the adjustment to the methods text as suggested above, and is repeated at line 576 for clarity.*

Line 432: Basically repeats something you have said in 360 and in 226. Just say it once, with maximum impact.

Response: *Left in to re-iterate point*

FIGURE 2: In the caption, mention green ulva (from line 120)

Response: *Figure caption adjusted to include reference to Ulva.*

FIGURE 3: Fix the missing bit of the formula. Shift the Rtk data panel somewhere else or at least change the background colour, because as drawn it looks like part of the conceptual panel.

Response: *Formula text box adjusted to reveal full formula. Thanks to the reviewer for the comment regarding the RTK panel. This is now changed to an alternate colour to remove confusion.*

FIGURE 4: Not really correct. Why is an equation shown on Figure 3 but not on Figure 4? Surely XC/D_NIWA_LINZ is measured from MLWS??

Response: *Figure 4 is correct. XC/D_NIWA_LINZ is estimated, not measured.*

FIGURE 6: Caption - note that no lidar comparison was produced for Kaikoura harbour. Even better, show the real picture with appropriate error bars.
Response: *Discussed above, no data was available*

FIGURE 7: part b - No Rainbow, not now, not ever. Use a proper colour stretch, and stretch it over the elevation range from sea to just above the road. I don't particularly care about the hill.
Response: *Clearly this is a personal preference. There are no standards for colour ramps and we feel comfortable with the Figure as it stands.*

References:
Quigley, M.C., Hughes, M. W., Bradley, B.A., Ballegooy, S.v., Reid, C., Morgenroth, J., Horton, T., Duffy, B., and Pettinga, J.R.: The 2010-2012 Canterbury earthquake sequence: Environmental effects, seismic triggering thresholds and geologic legacy, Tectonophysics, 672-673, 228-274, 2016.

Reid, C. M., James, N. P., and Bone, Y.: Carbonate sediments in a cool-water macroalgal environment, Kaikoura, New Zealand, Sedimentology, 58, 1935-1952, 2011.

Reviewer≠2: Anonymous

Dear editor,

Thank you for giving the opportunity to review the paper by Reid et al.

I read with interest the submitted manuscript and overall I believe it is an interesting contribution fitting the scope of the journal.
The authors use tidal data and the ecological preference of intertidal algae to determine coastal uplift. They calibrate their biological data with both real-time and predictive tidal charts and compare their results with lidar and strong motion data. Overall, I think their proposed methodology will be of interest to many coastal geomorphologists and geologists working with coastal deformation and their paper deserves publication.
We thank the reviewer for the positive comments.

However, in order for their methodology to be replicated some revisions are necessary, primarily in the methods section. In particular, paragraphs 3.2.1 – 3.2.3 are quite hard for a reader to follow and more complicated that necessary. I suggest the authors to improve this part by explaining in a better way their methodological approach.
The manuscript has been clarified accordingly as a response to both reviewers' comments.

Some technical corrections:
line 376: include the error bar → *error is provided at line 559*
line 389-390: error bar for NIWA and LINZ? *error is provided at lines 574 and 575*
line 418: middle on line, "they" is not needed→ *Done.*
Caption of figure 1: line 570, note that the position of State Highway One is the yellow line → *Corrected.*
Figure 6: I would suggest to include error bars→ *Errors are presented in Table 5 as they are too small to be represented graphically.*

Using a calibrated upper living-position of marine-biota to calculate coseismic uplift: the case-study of 2016 Kaikōura Earthquake, New Zealand

Catherine Reid[1], John Begg[2], Vasiliki Mouslopoulou[3,4], Onno Oncken[4], Andrew Nicol[1], Sofia-Katerina Kufner[4,5].

[1]Department of Geological Sciences, University of Canterbury, Private Bag 4800, Christchurch 8140, New Zealand.
[2]GNS Science, PO Box 30-368, Lower Hutt, New Zealand
[3]National Observatory of Athens, Institute of Geodynamics, Lofos Nimfon, Athens, 11810, Greece
[4] GFZ Helmholtz Centre Potsdam, German Research Centre for Geosciences, Telegrafenberg 14473, Potsdam Germany
[5]British Antarctic Survey, High Cross, Madingley Rd, Cambridge CB3 0ET, United Kingdom

Correspondence to: Vasiliki Mouslopoulou (vasiliki.mouslopoulou@noa.gr)

Abstract. The 2016 M_w 7.8 Kaikōura Earthquake (South Island, New Zealand) caused widespread complex ground deformation including significant coastal uplift of rocky shorelines. This coastal deformation is used here to develop a new methodology, in which the upper living limits of intertidal marine biota have been calibrated against tide-gauge records to quantitatively constrain pre-deformation biota living-position relative to sea level. This living-position is then applied to measure coseismic uplift at three other locations along the Kaikōura coast. We then assess how coseismic uplift derived using this calibrated biological method compares to that measured using other methods [Light Detection and Ranging (LiDAR) and strong motion data], as well as non-calibrated biological methods at the same localities. Data show that where biological data is collected by RTK-GNSS in sheltered locations, this new tide-gauge calibration method estimates tectonic uplift with an accuracy of +/- ≤0.07 m in the vicinity of the tide-gauge, and an overall mean accuracy of +/- 0.10 m or 10% compared to differential LiDAR methods for all locations. Sites exposed to high wave wash, or data collected by tape-measure, are more likely to show higher uplift results. Tectonic uplift estimates derived using predictive tidal charts produce overall higher uplift estimates in comparison to tide-gauge calibrated and instrumental methods, with mean uplift results 0.21 m or 20% higher than LiDAR results. This low-tech methodology can, however, produce uplift results that are broadly consistent with instrumental methodologies and may be applied with confidence in remote locations where LiDAR or local tide-gauge measurements are not available.

Deleted: A new method for calibrating marine biota living-depth position using the 2016 Kaikōura Earthquake uplift¶

Deleted: depths

Deleted: depth

Deleted: biologically measured tectonic uplift

Deleted: also test

Deleted: tectonic

Deleted: measured

Deleted: marine biota

Deleted: vertical deformation

Deleted: ,

Deleted: at the same localities, using instrumental methods [Light Detection and Ranging (LiDAR) and strong motion data],

Deleted: nd

Deleted: ight

Deleted: satellite data

1 Introduction

Vertical displacement has been measured globally using inter-tidal marine biota on rocky coastlines which often provide important constraints for incremental uplift during large-magnitude earthquakes and cumulative geological uplift (e.g. Alaska: Plafker, 1965; California: Carver et al., 1994; Mexico: Bodin and Klinger, 1986; Ramirez Herrera and Orozco 2002; Costa Rica: Plafker and Ward 1992; Chile: Fitzroy, 1839; Castilla, 1988; Castilla et al., 2010; Farias, 2010; Vargas et al., 2011; Melnick et al., 2012; Argentina: Ortlieb et al., 1996; Eastern Mediterranean: Pirazzoli et al., 1982; Stiros et al., 1992; Laborel and Laborel-Dugeun, 1994; Mouslopoulou et al., 2015a; Japan: Pirazzoli et al., 1985 and New Zealand: Mouslopoulou et al., 2019). Biological data was the basis for the first written records of coastal uplift following earthquakes along the Chilean coast (Graham, 1824; Fitzroy, 1839; Wesson, 2017) and continue to provide important constraints for elastic rebound and coseismic slip processes together with the locations, depth and dip of causal faults (e.g., Melnick et al., 2012; Wesson et al., 2015; Mouslopoulou et al., 2015b; 2019).

Biological indicators such as lithophagid borings and stranded bioconstructions of corals, coralline algae and barnacles, along with brown algae, gastropods, bivalves, and additional intertidal species with locally reliable tidal elevation zones, have been used to estimate eustatic sea-level changes and rock uplift (or subsidence) due to tectonic processes (Laborel and Laborel-Dugeun, 1994). Quantifying earthquake uplift from such biological datasets has been achieved using a variety of techniques, from simple measuring devices, such as tape measures, to laser survey methods and Global Navigation Satellite System (GNSS) techniques. While some studies (e.g., Melnick et al., 2012; Jaramillo et al., 2017) have successfully compared the reliability of the conventionally acquired biological uplift records against Real Time Kinematics (RTK) GNSS measurements, none have attempted to numerically and independently quantify the living-position of each biological marker. Jaramillo et al. (2017) compare pre- and post-deformation intertidal biota, but most studies, including this one, rely on post-deformation data only. Clark et al. (2017) and Mouslopoulou et al., (2019) use a variety of methods to record deformation immediately following the 2016 Kaikōura Earthquake, however, their marine-biota measurements have not previously been calibrated. Moreover, none of the above studies have systematically compared the manually collected tape-measurement estimates of coseismic uplift with instrumental earthquake-uplift datasets at individual localities to quantitatively assess the potential uncertainty inherent in the various techniques.

In this paper we use uplift produced by the November 14th, 2016 7.8M_w Kaikōura Earthquake (South Island, New Zealand) to develop a methodology for calibrating coastal vertical deformation utilising the displacement of biological marker horizons near a local tide gauge site. This calibrated information can then be applied to estimating coastal uplift or subsidence at other sites in the Kaikōura region. Capitalising on the long-term, continuous, high-precision tide-gauge readings at Kaikōura Peninsula, biological markers within the intertidal zone uplifted during the earthquake are here utilised to: a) develop a new methodology with which to independently calculate (and thus calibrate) the upper living-position of

Deleted: Clark et al., 2011;
Deleted: offered
Deleted: depth
Deleted: measuring
Deleted: vertical
Deleted: biozones
Deleted: indicators of
Deleted: most
Deleted: depth

individual intertidal (algal) taxa (organisms which are widely used to measure coseismic vertical displacement), and; b) compare, at each of three localities, the conventional biologically constrained hand-held measurements of coseismic uplift to values derived using various real-time remote sensing and other instrumental techniques, such as RTK-GNSS, LiDAR and strong-motion seismometers. Results may have application to inform future studies of the reliability of biological uplift measurements along rocky shores arising from large earthquakes at mid-latitudes (particularly in the Southern hemisphere) and with moderate tidal ranges (e.g., ~2 m), especially where instrumental technologies, such as differential LiDAR, are not available.

2 Geological and biological setting

2.1 The 2016 Kaikōura Earthquake

The 2016 M_w 7.8 Kaikōura Earthquake ruptured across the southern end of the Hikurangi subduction margin in northeastern South Island of New Zealand (Mouslopoulou et al., 2019). Northeast of the Kaikōura Earthquake surface rupture, the plate boundary is dominated by oblique subduction of the Pacific Plate beneath the Australian Plate at rates of 40-47 mm/yr (De Mets et al., 1994) (Fig. 1, inset). At the southern termination of the subduction, relative plate motion is transferred onto the transcurrent Alpine Fault via strike-slip on the Marlborough Fault System (MFS) (Pondard and Barnes, 2010; Wallace et al., 2012). The MFS generally strikes parallel to the relative plate motion vector and these active faults mainly accommodate right-lateral strike-slip with the amount of fault-related uplift increasing towards the coast. Offshore and east of the surface rupture, plate boundary deformation manifests itself as an accretionary prism complex. The accretionary complex and eastern MFS are underlain by the Pacific plate which, based on the presence of a Wadati-Benioff Zone, extends to a depth of at least 200 km beneath the northern South Island (Eberhart-Phillips and Bannister, 2010). The subducting slab is at a depth of ~20-30 km beneath the surface fault traces at Kaikōura (Nicol et al., 2018) and ruptured in response to slip triggered by these surface-breaking faults during the earthquake (Mouslopoulou et al., 2019).

The Kaikōura Earthquake is the largest (M_w=7.8) historic earthquake to have ruptured within the southern termination of the Hikurangi subduction margin (Mouslopoulou et al., 2019). The earthquake involved a complex network of at least 21 strike-slip, thrust and oblique-slip upper-plate faults that ruptured the ground surface and straddle the coastline of the northeast South Island (Hamling et al., 2017; Litchfield et al. 2018). The event's complexity is reflected in the moment tensor of the main shock which features only 65 to 75% double couple percentage (GEOFON http://geofon.gfz-potsdam.de accessed March 20, 2017) and is characterized by an oblique mechanism, with components of thrusting and right-lateral slip. Fault ruptures generally propagated northwards from the epicentre for about 200 km, with a focal depth of the main shock at 15 km (Hamling et al., 2017; Kaiser et al., 2017; Cesca et al., 2017). The resulting surface ruptures vary in strike from east-west to north-northwest with faults having east-northeast strike being primarily right-lateral strike-slip and more northerly striking

Deleted: individual
Deleted: four
Deleted: estimates
Deleted: acquired by
Deleted: surface
Deleted: faults
Deleted: , upper
Deleted: crustal
Deleted: comprised
Deleted: Clark et al., 2017;

faults accommodating strike-slip and reverse displacement (Nicol et al., 2018). The earthquake ruptured three faults (Hundalee, Papatea and Kekerengu faults) that cross the coastline and locally produced differential uplift of the rocky shorelines. Vertical displacement of -0.5 to +8 m occurred along >100 km of coastline with the highest values in the hanging wall of the reverse sinistral Papatea Fault north of Kaikōura (Litchfield et al. 2018; Mouslopoulou et al., 2019). The coastal section examined in this paper is crossed by the Hundalee Fault (Fig. 1; see also Figure 1c in Mouslopoulou et al., 2019) which accommodated a component of reverse displacement and uplift of the coast up to ~2 m. In addition to the mapped surface faults, the spatial extent of coastal uplift and the widespread occurrence of tsunamis (which propagated distances of up to ~250 km from Kaikōura south; Power et al., 2017) and the significant afterslip on the plate-interface, suggest that faulting at the ground surface was accompanied by slip on the subduction interface and an offshore thrust fault that splays from the plate-interface to extend within the accretionary prism complex (e.g., Cesca et al., 2017; Mouslopoulou et al., 2019).

2.2 Physical and Biological Setting

The northern Canterbury coastline is predominantly exposed to wave action, strikes northeast-southwest, and is broken only by the promontory of the Kaikōura Peninsula (Fig. 1). Hinterland topography is steep and the coastal strip is narrow, comprising mainly greywacke bedrock beneath bouldery shorelines interrupted by bays with gravel-dominated beaches. Prevailing winds from the northeast (summer months) and southwest (winter months) maintain year round exposure and the coastline supports a biota adapted to this high energy setting. The region is in a cool temperate oceanographic setting with semi-diurnal tides with a daily tidal variation of ~2 m. These factors influence the living positions of intertidal biota.

The intertidal biota in this cool temperate setting is dominated by seaweeds, typically the large brown algae *Durvillaea antarctica* (bull-kelp), *D. willana*, *Carpophyllum maschalocarpum* (Fig. 2a), and *Hormosira banksii*, coralline algae (Fig. 2b), barnacles, limpets, chitons and mobile invertebrates (Marsden, 1985). Attached invertebrates, such as mussels and oysters, are present but not common on this stretch of coast. On the Kaikōura Peninsula species diversity is high, with up to 78 species present in a single intertidal transect (Marsden, 1985). The vertical distribution of species on these rocky shores is controlled by exposure to wave action as well as interspecies competition (Goldstien pers. comm., 2017). The rocky shores around Kaikōura support three major biozones that approximately correspond to tidal height: a) an upper belt of littorinid gastropods (e.g., *Littorina unifasciata* and *L. cincta*) and barnacles (e.g., *Epopella plicata*); b) a mid-tidal region dominated by grazing molluscs (e.g., *Cellana denticulata, Melagraphia aethiops* and *Turbo smaragdus*); and c) a lower zone of brown algae (e.g., *Durvillaea antarctica* and *Carpophyllum maschalocarpum*) (Marsden, 1985). When the shoreline was inspected, about two and a half months after earthquake uplift, many mobile taxa were absent in the uplifted intertidal zone and living or dead remains of stranded encrusting or attached taxa, such as barnacles, coralline algae and brown algae, dominated the shoreline. The green alga *Ulva* is normally present in limited amounts (Marsden, 1985), however, following the Kaikōura

Deleted: Clark et al., 2017;

Deleted: ,

Deleted: ,

Deleted: span

Deleted: (

Deleted: may have been

Deleted: probably

Deleted: and

Deleted: exposing

Deleted: which are

Deleted: jus

Deleted: . D

Deleted: is up to

Deleted: ,

Deleted: which in turn

Deleted: s

Deleted: depths

Deleted: Encrusting

Earthquake and shoreline disturbance, growth of this alga was prolific and it subsequently covered much of the post-earthquake intertidal zone in the study area (Fig. 2b-d). This proliferation was accompanied by the death and bleaching of stranded coralline red algae forming a distinctive white crust on rocky surfaces (Figs. 2b & d), which were often visible at kilometre-scale distances; at that time, this was the most obvious visual indicator of uplift along the coastline.

In this study the brown algae *Durvillaea* and *Carpophyllum* are utilised to measure coastal uplift. *Durvillaea* is restricted to the southern hemisphere and occurs on rocky coastlines throughout New Zealand, while *Carpophyllum* is endemic (Adams, 1994). Around the Kaikōura Peninsula and north Canterbury coast, holdfasts of *Durvillaea antarctica* (bull-kelp) and *D. willana* (Fig. 2a), are anchored by a fleshy non-calcified holdfast to coralline encrusted rocky surfaces in the lower inter-tidal zone (Adams, 1994; Nelson, 2013) and holdfasts extend sub-tidally by 1-2 m. Individual plants have fronds 3-5 m in length that typically drape down from the inter-tidal zone to depths of ~5 m (Adams, 1994; Nelson, 2013). On sites exposed to higher wave action, holdfasts of *Durvillaea* may appear higher in the intertidal zone due to increased wave wash (Marsden, 1985), however, in sheltered areas and sites where waves are baffled holdfasts may be sub-aerially exposed at spring low tides, but not at neap low tides (Goldstien pers. comm., 2017). By contrast, *Carpophyllum* is only present in the low intertidal zone where it forms a distinct band close to low water (Nelson, 2013) (label *C* in Fig. 2c), and is not normally emergent at low spring tides (Goldstien pers. comm., 2017). Although both *Carpophyllum* and *Durvillaea* may be present on open coasts (Fig. 2a), *Durvillaea* dominates in exposed sites and *Carpophyllum* is more abundant at relatively sheltered locations. Dead stranded, and living representatives of one or both of these brown algae were present at all the rocky coastal sites visited in this study, making *Carpophyllum* and *Durvillaea* an excellent combination of biozone markers for measuring coseismic uplift.

The reproductive season for *Durvillaea* is during the winter months peaking in August and harvesting studies have shown slow resettlement when fronds are removed in September through February (Hay and South, 1979). The intertidal zone on the Kaikōura coast is undergoing recovery from the November 2016 earthquake and stabilised intertidal zones are not yet re-established. In temperate climate settings this may take several years, as shown by Castilla and Oliva (1990) following the 1985 Chile earthquake.

3 Methods

To measure coseismic uplift due to the Kaikōura Earthquake, independent methods utilising marine biological sea-level indicators, tidal gauge measurements, remote sensing techniques (RTK-GNSS and LiDAR) and strong motion recordings are used. The characteristics of each dataset collected and the methodology used to derive tectonic uplift are presented below. All uplift data are available in the Supplementary Material.

Deleted: and
Deleted: were
Deleted:
Deleted: in response
Deleted: at
Deleted: exposed
Deleted: seen
Deleted: One

3.1 Kaikōura Tide Gauge

New Zealand has 15 tide-gauges which record tidal variation, tsunami events, eustatic sea-level changes and vertical displacements of the coast. The Kaikōura Tide Gauge (Fig. 1) measures sea-level relative to two Druck PTX1830 sensors (KAIT 40 and 41 each referenced to different datums) located at the end of the wharf at Kaikōura (WGS-84 -42.41288°, 173.70277°; NZTM 1657824, 5304141). In this study, data from the KAIT 41 sensor (http://apps.linz.govt.nz/ftp/sea_level_data/KAIT/) are used exclusively to maintain internal consistency, although results would be the same had KAIT 40 been used. The instrument is fixed to bedrock beneath the wharf, referenced to nearby benchmarks, including one on the wharf itself (LINZ geodetic code EEFL) and records sea-level at one minute intervals. The data are recorded in UTC time and the water-levels represent water surface elevation above the base of the tide-gauge in metres. The tide-gauge was established in late May 2010 and operated continuously through the period of the November 14th Kaikōura Earthquake recording tectonic uplift at the site. KAIT 41 Tide Gauge data assembled for this study spanned the period from December 1st, 2015 to February 7th, 2017 and indicate that tidal range varies between a spring tide average of c. 2 m and c. 1.25 m during neap tides (Table 1). Spring low-tides before the Kaikōura Earthquake registered c. 2.05 m on the gauge while spring high-tides were c. 4.05 m. After the earthquake, low-water spring tide measured c. 1.1 m and high-water spring c. 3.1 m. Neap tides measured c. 2.5 m (low) and c. 3.7 m (high) before the earthquake and c. 1.5 m (low) and c. 2.75 m (high) after the earthquake (Table 1).

To determine the absolute uplift value from the tide-gauge data (U_{TG}; see Suppl. File S1) we used the following methodology: A) Subtracted the high-spring and high-neap tide readings before the earthquake from those after the earthquake; B) Averaged high-tide and low-tide readings from several tidal cycles (3 day period) before and after the earthquake; C) aligned pre-earthquake tidal data with post-earthquake data and incrementally adjusting them until achieving a best fit; D) compared the average water elevation from a pre-earthquake month to the same month's data after the earthquake (e.g. December 2015 against December 2016); and E) calculated the difference in average waterline elevations for an extended period (44 days) before and after the earthquake (Oct. 30th to Dec. 27th). The average uplift (U_{TG}) estimated from the above steps (Tables 1 & 2) is subsequently used to independently estimate the pre-earthquake upper range of the species used in this study (see Sect. 3.2). It has also acted as a reference point against which all other instrumental and hand-held measurements are compared.

Some limitations on calculating vertical displacement from tide-gauge records arise from the specific circumstances associated with the record around the November 14th, 2016 M_w 7.8 Kaikōura Earthquake. This event struck during a period of sharply increasing tidal change due to high spring tides (related to lunar perigee and approaching solar perihelion) that culminated a few days after the earthquake. In addition, the earthquake generated a significant tsunami (Power et al., 2017), the effects of which persist in the tide-gauge record for at least 12 hours after the earthquake. Further, a day after the

Deleted: motion
Deleted: however,
Deleted: a
Deleted: b
Deleted: c
Deleted: d
Deleted: e
Deleted: ferred dwelling
Deleted: biological holdfast
Deleted: e

earthquake, Kaikōura was subjected to a southerly storm with powerful swells and these are also apparent in the tide-gauge data. These factors result in some blurring in the precision of uplift deriving from the difference between pre-earthquake and post-earthquake data.

Uplift values calculated from tide gauge data were compared with those derived from LiDAR differencing data (see Section 3.4.1). Biological data from this site (see Section 3.2) were used to calibrate the elevation of the upper extent of brown algal holdfasts relative to sea level (in this case, MLWS).

3.2 Biological Data Collection

Biological data collected comprised the location and elevation of approximately 400 stranded algal holdfasts during a ten-day period, approximately two and a half months after the Kaikōura Earthquake (Suppl. File S2). Decay of attached and uplifted biota was well-advanced and, in most cases, uplifted remnants of marine algae, our primary target species, were restricted to holdfast stumps of *Durvillaea* or *Carpophyllum* with brittle fronds attached (Figs. 2b-d). Despite the decay of algae, the position of the remaining stumps clearly reflected pre-earthquake algae distribution evidenced by a lack of rock "scarring" where removed stumps might also remove other intertidal biota and often expose fresh rock surfaces. The biological data presented in this paper were collected from close to the Kaikōura Tide Gauge on the northern side of the peninsula, Kaikōura Harbour on the south side, and from two localities along the south Kaikōura coastline, Paia Point and Omihi Point (Fig. 1).

At all localities uplift was apparent from the exposure and subsequent degradation of intertidal biota with algal holdfasts exposed above the waterline, and measurements were collected on rising or falling mid- and low-tides. Holdfasts were preferentially measured on rock faces sheltered from, but retaining connection to, the open sea, to minimise error introduction by the potentially higher tidal position of *Durvillaea* in wave-washed sites. Each site was visually assessed to establish the upper extent of holdfasts, and the upper holdfasts were measured (as they represent specimens closest to the pre-earthquake upper limit for each species). In sites with boulders rather than bedrock exposure, only boulders that showed a portion of their surface to have been clearly within the pre-earthquake mid- or upper-tidal zone (evidenced by bare or barnacle encrusted surfaces) and had clearly remained undisturbed by strong ground shaking and subsequent storm wave exposure were selected for measurement, therefore ensuring the upper limit of holdfasts were represented.

Two different methods were used to measure the vertically displaced biota. The primary method of collection of field data was by Real Time Kinematic Global Navigation Satellite System (RTK GNSS). At each site the water-level was measured in the most sheltered area available to minimise wave effects, and the time the measurement was collected was recorded.

Deleted: data

Deleted: records of coseismic uplift were

Deleted: using

Deleted: will be

Deleted: of

Deleted: independent

Following measurement of the waterline, up to twenty holdfasts (either or both *Carpophyllum* and *Durvillaea*) were measured within close proximity. Where additional holdfasts were available at each site water-level was re-measured and further sets of up to twenty holdfasts measured. This RTK collection method did not require the waterline measurement site and the holdfasts to be immediately adjacent to each other. Additional biological data were collected using a second method, direct tape-measurement of the height of holdfasts above water-level. Tape measurements were collected between the waterline (measured between wavelet peaks and troughs) and the upper algal holdfasts on rock surfaces. Sheltered faces were again preferentially measured, although the requirement to have stranded holdfasts immediately adjacent to a measurable waterline meant that sites exposed to wave-wash were more commonly used to achieve approximately twenty measurements. Each reading for both methods (RTK or tape) was annotated with the alga species measured and relative site exposure (exposed or sheltered) and time of measurement was recorded.

3.3 Biological Data Processing

These field measurements of holdfast heights were then processed to determine coseismic uplift, taking into account the time of data measurement within the tidal cycle and the pre-earthquake living position of algal holdfasts. Three different methods were used for calculating tectonic uplift from the vertical offsets of the biological horizons. These were: a) tide-gauge calibration, b) NIWA tide-forecaster measurement and, c) LINZ tide-prediction charts. The first method utilised data from the Kaikōura Tide Gauge and differs significantly from the two tide-prediction methods by calibration to real-time water-level records of the Kaikōura Tide Gauge. The NIWA forecaster and LINZ tidal chart methods are included, however, to simulate locations where real-time tide-gauges are not available. All data and calculations are presented in the Supplementary File S2.

3.3.1 Deriving an upper living-position correction using the Kaikōura Tide Gauge ($X_{C/D/G}$)

This new method determines an upper living-position for each species using the measured elevations of the stranded holdfasts and then relating them to the pre-earthquake tidal cycle (Fig 3) by subtracting uplift recorded by the tide-gauge. This enables the elevation of the holdfasts, which are being used to determine surface uplift, to be referenced to a pre-earthquake datum, in this case the base of the tidal cycle mean low water spring (MLWS). The Kaikōura Tide Gauge provides a record of the pre- and post-earthquake MLWS. First the height of the stranded holdfast is determined by adding the waterline height measured in the tide gauge (H) and the observed height of the holdfast above the waterline in sheltered locations (OM). The offset of MLWS pre- and post-earthquake in the tide-gauge calculated as uplift is subtracted, along with the height of MLWS in the tide gauge. This leaves a residual height that reflects the pre-earthquake elevation of holdfasts of each species with respect to MLWS.

The upper holdfast living-position is described here by the correction $X_{C/D}$, which is treated as a constant for *Carpophyllum*

Deleted: ,
Deleted: however,
Deleted: needed to be
Formatted: Heading 3
Deleted: apparent
Deleted: uplift
Deleted: further
Deleted: the total
Deleted: surface
Deleted: biota
Deleted: 2
Deleted: -depth
Deleted: factor
Deleted: seeks to
Deleted: depth
Deleted: and
Deleted: positions
Deleted: relative to
Deleted:
Deleted: depth
Deleted: factor

(X_C), *Durvillaea* (X_D) or a combination of both (X_G), respectively. $X_{C/D/G}$ were determined by the Eq. (1):

$$X_{C/D/G} = (H_{TG} + OM_{C/D/G}) - U_{TG} - MLWS \quad (1)$$

where H_{TG} is the waterline height at the tide-gauge at the time of data collection (which can be accessed from http://www.linz.govt.nz/ and which was averaged here over 10 min intervals to mitigate local fluctuations); $OM_{C/D/G}$ is the observed height above the waterline for each stranded holdfast (determined by subtracting RTK waterline height measurement from each RTK holdfast measurement per site, or directly using tape-measurements; the subscripts C/D/G correspond to measurements for the different holdfasts); MLWS is the average tide-gauge reading for mean low water-spring tide (1.1 m for KAIT 41; see Table 1); U_{TG} is this uplift calculated at the tide-gauge by the method described in Sect. 3.1.

As *Carpophyllum* and *Durvillaea* occupy slightly different upper living positions in the inter-tidal zone, $X_{C/D}$ was calculated separately for each species. A general correction X_G, using both *Carpophyllum* and *Durvillaea* holdfasts was also determined, to be applied at sites where holdfast species were not known or determined, or insufficient numbers of each were available and data were pooled by necessity. To calculate the correction, data were pooled by species irrespective of site. The method described here uses the upper extent of intertidal algae as marker horizons, as at Kaikōura these are readily available attached biota. However, biozone boundaries for any attached inter-tidal organism with a restricted tidal range could be used to calculate this correction factor.

3.3.2 Deriving tectonic uplift using the Kaikōura Tide Gauge method ($U_{B(TG)}$)

Once the $X_{C/D/G}$ correction was derived as described above, coseismic uplift was calculated from biological data pooled by site in the location studied, using Eq. (2):

$$U_{B(TG)} = ((H_{TG} + OM_{C/D/G}) - MLWS) - X_{C/D/G} \quad (2)$$

where $U_{B(TG)}$ is the uplift calculated from biological data, at the Kaikōura Tide Gauge.

3.3.3 Deriving tectonic uplift using the NIWA Tide Forecaster ($U_{B(NIWA)}$)

In order to calculate uplift from sites distant to the tide-gauge RTK biological data was used in conjunction with tidal charts (https://www.niwa.co.nz/services/online-services/tide-forecaster) that provide tidal predictions for sites between formal chart stations and attempt to account for local variation. For this calculation, Eq. (3) is used:

$$U_{B(NIWA)} = (H_{NIWA} + OM_{C/D/G}) - X_{C/D\_NIWA}, \quad (3)$$

Deleted: (
Deleted: H
Deleted:)
Formatted: Subscript
Deleted: of
Deleted: indices
Deleted: prefer
Deleted: determined
Deleted: factor
Deleted: Further, only sheltered sites nearest the Kaikōura Tide Gauge were used to determine $X_{C/D/G}$.
Deleted: factor
Deleted: species
Deleted: locations
Deleted: with
Deleted: other
Deleted: biota
Deleted: 2
Deleted: factor
Deleted: H
Deleted: OM
Deleted: 2
Deleted: Uplift was also calculated from
Deleted: ing
Deleted: OM+

where $OM_{C/D/G}$ is the observed elevation of the holdfasts relative to locally measured sea level, H_{NIWA} is the predicted tide height from NIWA charts at the survey time, and X_{C/D_NIWA} is a correction value (NIWA Forecaster calibrated correction), estimated to reflect the relative height of *Carpophyllum* and *Durvillaea* within the tidal cycle (Fig. 4). This value for X is independent of tidal-gauge data as used above and relies on assessment of qualitative biological data only. As described in Sect. 2.2, *Carpophyllum* in sheltered areas with connection to the sea will not usually be exposed at low spring tide (LST) (Goldstien pers. comm., 2017). Tidal prediction charts over one year were qualitatively assessed and a mean low spring tide height of 0.1 m (X_{C_NIWA}) estimated for the upper limit of *Carpophyllum* and used as the correction value for this species in data processing. Likewise *Durvillaea* will be regularly exposed at low spring tides but usually not exposed at low neap tide (Goldstien pers. comm. 2017). A correction (X_{D_NIWA}) of 0.25 m was estimated, representing a height between spring and neap low tides, relevant to the Kaikōura region. These values for X_{C/D_NIWA} assume the upper holdfast elevation of *Carpophyllum* and *Durvillaea* are consistent between sheltered and exposed areas.

Deleted: (Fig. 4)

Deleted: 3

Deleted: regional

Deleted: height

Deleted: tant

Deleted: in both

The value H_{NIWA} was determined using the predicted tide heights and times from the NIWA Tide Forecaster website. The NIWA Tide Forecaster provides tide height at user designated locations, that may be between the fixed LINZ locations in order to accommodate the passage of tidal highs and lows between fixed points. H_{NIWA} was calculated using the following Eq. (4) from http://www.linz.govt.nz/

Deleted: .

$$H_{NIWA} = h1 + (h2 - h1)\,[(\cos A + 1)/2] \quad (4)$$

Where $A = \pi([(t - t1)/(t2 - t1)] + 1)$ radians and t1 and h1 denote the time and height of the tide (high or low) immediately preceding time t, and t2 and h2 denote the time and height of the tide (high or low) immediately following time t. Only time t is measured, t1 and t2 and h1 and h2 are derived from predictive tide charts.

3.3.4 Process to derive tectonic uplift using the LINZ tide prediction charts ($U_{B(LINZ)}$)

Deleted: 2

Land Information New Zealand (LINZ) tide charts available at http://www.linz.govt.nz/ provide fixed tide prediction charts for New Zealand primary and secondary ports and were also used to derive H_{LINZ}, using Eq. (3), and LINZ calibration correction values of 0.2 m for X_{C_LINZ} and 0.4 m for X_{D_LINZ} estimated as above from these charts. H_{LINZ} was again determined by Eq. (4) defined above, and only RTK data was processed this way.

3.3.5 Sources of error

Data points collected by RTK GNSS were accurate to ± 5 cm, and this applies to both the waterline measurement at each site, and each holdfast measurement. Both of these measurements were used to derive OM, with a total error of ± 10 cm. Manually-collected biological data rely on the accuracy of the waterline measurement taken. While sheltered microsites were selected for these measurements, they were placed at an estimated median water-level between wavelets. This error is more pronounced when measuring waterline heights at more exposed sites. Additionally the time at which the measurement was taken may have occurred when water-level was at either a positive or negative fluctuation from tidal prediction charts or Tide Gauge readings for sites south of Kaikōura. The total error is difficult to quantify, however, assessment of the Kaikōura Tide Gauge data show water-level fluctuations of less than +/- 0.1 m. Averaging tide-gauge data over 10 minutes helped mitigate the error resulting from the tide gauge itself, however, the error introduced by sea-level fluctuations away from the tide-gauge remained.

Durvillaea lives along open coasts, however at very exposed sites pre-earthquake holdfasts would have sat higher than average in response to increased wave wash and run-up. This potential error is difficult to quantify as deviation from average heights will be linked to wave heights and run-up at individual sites that may be modified following uplift. For this reason, the most exposed sites were avoided (where possible) and data were collected from sheltered locations.

3.4 Differential LiDAR and strong motion uplift estimates

3.4.1 Differential LiDAR (U_{LiDAR})

Differential LiDAR has been developed along the coastal south Kaikōura region using pre- (DEM_Kaikōura_2012_1m) and post-earthquake (NZVD2016 and DEM_NZTA_1m) surveys of road and railway routes using a common geodetic datum for each survey. To minimise the impact of gravity-induced slope failures and horizontal tectonic displacement on sloping ground during the earthquake, the difference of the altitude of 1x1 pixels along the post-earthquake centreline of roads was used. Specifically, for the Omihi Point and Paia Point study localities (see Fig. 1) the nearby State Highway-1 was used, while for the Kaikōura Tide Gauge study-site, a section of the coastal road near the wharf that houses the gauge was used. The road sections that acted as a reference level have low relief (e.g., <10 cm relief) and are wider than the horizontal displacements recorded during the earthquake; thus, neither lateral tectonic displacement nor gravitational processes should significantly impact on the differential LiDAR measurements. Collectively, a total of 510 differential LiDAR points were collected and analysed (148 at the Kaikōura Tide Gauge, 152 points at Paia Point and 210 points at Omihi Point) (Suppl. File S3). These data were used to produce mean uplift estimates of at each site with 2σ uncertainties of ±0.06-0.18 m (Table 6). Differential LiDAR data was not available immediately adjacent to Kaikōura Harbour, on the south side of the peninsula.

Deleted: 2
Deleted: occurs
Deleted: at
Deleted: ,
Deleted: 3
Deleted: Remote sensing
Deleted: 3
Deleted: (Fig. 7)

3.4.2 Strong motion (U_{SM}).

A further independent instrumental uplift measurement was achieved by calculating the static vertical displacement recorded by the nearby strong-motion site KIKS (Fig. 1). The KIKS station is located 2.2 km south of the Kaikōura Tide Gauge (lat./long. -42.426°N/173.682°E; NZTM: 1656161, 5302714; see Fig. 1) and operated by GeoNET. The Kinemetrics FBA-ES-T-BASALT 2420 sensor is located at 8 m elevation on the concrete floor of a single storey building at Kaikōura Harbour. Ground acceleration is recorded with a period of 0.005 s and data can be downloaded online from ftp://ftp.geonet.org.nz/strong/processed/.

Static displacement was calculated from the vertical component of the instrument following the method of Wang et al. (2011) and using their software package *smbloc*, which applies an empirical baseline correction to remove linear pre- and post-event trends in the data. Static displacement derived with this method after large earthquakes has been shown to be robust (e.g. Schurr et al., 2012). Here, the resulting vertical displacement for the KIKS strong-motion station is 0.87±0.06 m (Table 6 & Suppl. File S4 for further details on data processing).

4 Results and comparison of methods

4.1 Kaikōura Tide Gauge locality

Tide gauge data indicate that the Kaikōura Tide Gauge was coseismically uplifted by 0.96 ± 0.02 m (U_{TG}) (Table 1 and 2) (see sect. 3.1) and represents a key reference point for this study. In addition to providing an independent estimate of uplift, the tide gauge data have been used to calculate the upper living-position correction factor $X_{C/D/G}$ from all stranded biological holdfast data collected proximal to the Tide Gauge (Eq. 1) (Table 3; Fig. 5).

The calculated corrections $X_{C/D}$ (Table 3) were applied to biological measurements collected proximal to the Kaikōura Tide Gauge (Fig. 5) and compared with uplift of the Kaikōura Tide Gauge (calculated in section 3.1). RTK-GNSS survey data of *Durvillaea* and *Carpophyllum* for sheltered and exposed holdfasts produce tectonic uplift values of 0.71 m to 1.13 m, with a mean of 0.97 m ± 0.08 m (Table 4, Fig. 5). Similarly, for all tape-measure data collected proximal to the tide gauge, tectonic uplift estimates range between 0.87 m and 1.35 m, with a mean of 1.05 ± 0.11 (Table 4, Fig. 5). The resulting analysis suggests *Carpophyllum* at sheltered sites recorded using RTK-GNSS and tape measure produce uplift estimates that are, within the uncertainties given, indistinguishable from uplift recorded by the tide-gauge (0.96 m) and differential LiDAR (0.92 cm) (Fig. 5). By contrast, estimates of uplift using *Durvillaea* are always higher than tide-gauge and differential LiDAR values. Tape-measurements of *Durvillaea* produced the highest biological uplift estimates with exposed *Durvillaea* recording a mean uplift of 1.21 m, which is 0.25-0.29 m above the tide-gauge and differential LiDAR values (Table 4, Fig.

Deleted: 3

Formatted: Heading 2

Deleted: he

Deleted: -

Deleted: depth

Deleted:) and test this method at the Kaikōura Tide Gauge (

Deleted: Uplift estimates derived from direct tide-gauge analysis (i.e., the method described in Sect. 3.1), are here compared to uplift estimates derived from biological methods (Equations 2 & 3 in Sect. 3.2) (Fig. 6a).

Deleted: factors

Deleted: estimates based on

5). These data suggest that *Durvillaea* should be regarded as providing maximum uplift estimates, supporting previous work in suggesting that *Durvillaea* at exposed sites should be used with caution (e.g., Clark et al., 2017).

The same biological data collected near the Kaikōura Tide Gauge was then grouped by data collection location (sets of approximately twenty data points) rather than holdfast type, and uplift estimates produced results of 0.99 m ± 0.07 m, 0.923 m ± 0.10 m and 0.98 m ± 0.07 m, while tape measures resulted in uplift estimates of 1.00 m ± 0.07 m, 1.12 m ± 0.11 m and 1.19 m ± 0.08 m, respectively (Fig. 6a, Table 5). In addition to directly measuring water-levels at the tide-gauge, the NIWA Forecaster and LINZ tide-charts were used to calculate uplift in an effort to test the utility of tide-charts at remote locations where tide gauge and instrument data may not be available. These comparisons are illustrated in Table 5 and Figure 6. At the tide-gauge site, the LINZ Tide Chart produced, for *Carpohyllum*, uplift results 0.11-0.12 m greater than the tide-gauge method, while NIWA Forecaster chart produced uplift estimates of 0.04-0.05 m greater than the tide-gauge mean (Table 5). As was the case for the tide gauge calibration method, *Durvillaea* produced the greatest uplift at the tide gauge using the tide chart method, with average uplift values of 1.18 m and 1.24 m. In summary, uplift estimates calculated from *Carpophyllum* holdfasts processed using the NIWA Forecaster tide charts (rather than LINZ charts), are the most similar to direct uplift of the tide-gauge itself, to the tide-gauge biological results and to LiDAR (plus 0-0.25 m), promoting their use in circumstances where a tide gauge is unavailable. LINZ tide chart methods produced results within 0.32 m of other methods.

Deleted: in

Formatted: Heading 2

4.2 Kaikōura Harbour, Paia Point and Omihi Point

To further test the utility of the Kaikōura calibration method, and the other methods under consideration, algae uplift data were also processed from the Kaikōura Harbour, Paia Point and Omihi Point sites. Data from these locations are not as detailed as those collected at the tide-gauge study-site itself, with the distinction between *Carpophyllum* and *Durvillaea* or sheltered and exposed not always available.

At Paia Point, uplift estimates from all data collection and processing methods range from 1.12 m to 1.36 m, with a mean uplift of 1.24 m ± 0.16 m (Table 5; Fig. 6). While the biological uplift results are internally consistent, on average they are about 0.2 m higher than the differential LiDAR average uplift at this site, which is 1.05 m ±0.07 m (Table 6; Fig. 7). This higher estimate for biological data cannot be attributed to differences in species of algae or measurement technique, however, shoreline exposure to wave action cannot be excluded as a factor. The role of shoreline exposure may only be resolved once the uplifted shoreline is recolonised with new *Carpophyllum* and *Durvillaea*. Algal uplift measurements collected at Omihi Point (Fig. 1), and processed using the tide-gauge calibration correction $X_{C/D}$ are within 0.07 m from one another and to uplift recorded by differential LiDAR (Tables 5 & 6, Fig. 6). RTK measurements from Omihi Point processed using the NIWA Forecaster and LINZ tide charts methods are 0.08 m and 0.23 m respectively above tide-gauge calibrated estimates. In summary, there is no systematic difference in the uplift estimates at Paia and Omihi Points between the

Deleted: factor

different measurement techniques (RTK-GPS vs tape-measure), species of algae (*Carpophyllum* or *Durvillaea*) or tide charts (NIWA Forecaster or LINZ tide chart) (Fig. 6).

At the Kaikōura Harbour site, where the KIKS seismic station is located (Fig. 1), uplift estimates from biological data, processed with the tide-gauge calibrated upper living-position methodology are 0.74 m ± 0.12 m, 0.85 m ± 0.12 m for NIWA calibrated methods and 0.98 m ± 0.12 m for LINZ methods. These results bracket the uplift result recorded by the strong motion data of 0.87 m ±0.06 m (Fig. 6). Differential LiDAR was not available adjacent to Kaikōura Harbour for comparison with biological measurements.

Comparison of results for all biological methods, independent of location, shows a consistent correlation (Fig. 8). No single method stands out as producing persistently divergent results from other methods, although all biological methods produce uplift estimates that are higher than LiDAR results. The tide gauge calibrated method has yielded results most consistent to LiDAR. At all sites uplift estimated using the tide gauge calibration method give results within 0.0 to +0.21 m (or 0.35 to 21%) higher than LiDAR results, with a mean of +0.11 m (10%). Further, at all sites and over all biological methods, uplifts estimates are 0.0 to +0.31 m (or < 34%) higher than associated LiDAR results, with a mean of + 0.17 m.

5 Discussion

The distribution of kelp within the intertidal zone at Kaikōura is well defined with respect to qualitative upper, mid and low intertidal zones (Marsden, 1985). Nevertheless, because the width of the intertidal zone varies with site exposure, topography, wave-wash and competition between different organisms, an attempt to quantify this uncertainty is made by calibrating coseismically uplifted intertidal brown algae (*Durvillaea* and *Carpophyllum*) in the immediate vicinity of the Kaikōura Tide Gauge, aiming to establish a quantitative correction value for the upper living-position of the kelp holdfasts with respect to MLWS (Figs. 3 and 5).

Using Eq. (1) (see Sect. 3.2) at the Kaikōura Tide Gauge, an upper living-position correction of X_C of 0.26 ± 0.09 m above MLWS is derived for sheltered *Carpophyllum maschalocarpum*. For *Durvillaea* in sheltered sites, the upper living-position correction X_D is 0.38 ±0.09 m above MLWS. These values were subsequently used to estimate tectonic uplift at sites located up to 15 km from the tide-gauge and produced uplift measurements which were in good agreement with uplift calculated at the same localities by differential LiDAR (Figs. 6 and 7). Thus, it appears that this method of estimating correction values may be important as it provides, for the first time, an independent quantitative method for estimating the preferred upper living-position for intertidal biota with respect to MLWS. This method may be applied elsewhere to other intertidal biota in the vicinity of a tide-gauge. *Carpophyllum* is endemic to New Zealand while *Durvillaea* is widespread in the southern hemisphere. The derived corrections are specific to these taxa in the Kaikōura region which is characterised by a moderate

Deleted:
Deleted: depth
Deleted: At this locality,
Deleted: the
Deleted: of the
Deleted: with LiDAR has not been attempted as differential LiDAR data produced inconsistent results over short distances.
Deleted: zones of
Deleted: depth
Deleted: depth
Deleted: factor
Deleted: a
Deleted: depth
Deleted: factor
Deleted: of
Deleted: is derived
Deleted: water-depth
Deleted: of
Deleted: values
Deleted: at

tidal range. If these values are applied elsewhere, the uncertainty would be equal to the maximum correction value of 0.38 m. The three biological post-processing methods used to obtain uplift, all yield results which are, within uncertainties, similar to one another, meaning that any of these methods could be applied depending on the available tidal data at the site of interest. Analysis of all data suggest that hand-held measurements most often overestimate uplift, compared to results from RTK-GPS survey data.

In the vicinity of the Kaikōura Tide Gauge, biological results using the tide-gauge correction are most similar to non-biological methods. With increasing distance from the tide-gauge, this new method provides reliable results; nevertheless, other biological methods were comparable. Progression of daily tides is even and fluctuations from the expected tidal progression may occur over several minute intervals due to natural unevenness in the ocean surface caused by wind, barometric pressure and local topography (eg. Garrison, 2010). While the influence of this natural fluctuation for biological data collected proximal to the tide-gauge is well mitigated by use of real-time tide gauge water-level (H), away from the Kaikōura Tide Gauge this real time fluctuation is less able to be mitigated. Therefore, the NIWA and LINZ tidal chart calculations for H, and associated corrections may give equally accurate uplift estimates. Overall, the NIWA method produces results more consistent with non-biological methods than does the LINZ method. Despite this, data collected by RTK and processed using predictive charts, such as LINZ, may be used to calculate uplift estimates, and could be used with confidence in remote locations, or locations where other methods are not available.

This study has shown that instrumental and biological methods can produce comparable results; yet, in order to reduce uncertainty in the biological methods, the biota should have a living-position relative to an appropriate sea-level datum that is calibrated against real-time tide-gauge data. To this end, our study has provided a new calibration method to derive a correction for this upper living-position that can be applied globally where tide-gauge records are available. In circumstances where tide-gauge records are unavailable, the usage of predictive charts to process biological data may still be appropriate, accepting that uncertainties may be higher. The use of strongly anchored taxa such as algae may allow for data to be gathered either immediately or a period of time after deformation. The timeframe over which data could be recovered post deformation will depend on local conditions, seasons and anchoring strength of taxa utilised.

6 Conclusions

Tectonic deformation determined from uplifted intertidal biozone indicators produce results comparable with tectonic uplift recorded by the Kaikōura tide-gauge, remote-sense datasets (LiDAR and RTK-GPS) and strong-motion seismic data. Calibrating measured intertidal biological data to real-time tide gauge records gives results within an average 0.11 m of those derived from direct uplift of the tide-gauge, and localised differential LiDAR values. Uplift results from biological data,

Deleted: they
Deleted: ,
Deleted: with
Deleted: higher for tape-measure data than
Deleted: measurement
Deleted: factor
Deleted: the
Deleted: factor
Deleted: -depth
Deleted: wards this direction
Deleted: factor
Deleted: -depth
Deleted:

calibrated using predictive tidal charts, are as reliable as other biological and non-biological methods when distant to real-time tide-gauges, and are appropriate for use where differential LiDAR or other real-time remote-sensing datasets are not available. Results from this study indicate that *Carpophyllum*, an alga with a tightly defined upper intertidal limit, is the most reliable predictor of uplift at sheltered sites. *Durvillea*, an alga with a less well-defined upper intertidal limit, is less reliable, especially when measured at exposed sites. Biological data collected by RTK-GNSS gives the strongest overall comparison to non-biological methods of estimating uplift. Data collected by tape-measure may be reliable where sheltered sites are available but are likely to provide higher apparent uplift results in exposed locations, where intertidal biozone boundaries are blurred and elevated by wave fetch and exposure on sections of a rocky coastline.

Deleted: e

Deleted: ,

Deleted: give

Deleted:

Deleted: s

Author's contributions

All authors contributed to the research idea, data-collection during fieldwork and their subsequent analysis. The first draft of the manuscript was written by C.R. with the contribution of all co-authors. The final manuscript resulted from close collaboration of all co-authors.

Acknowledgements

This work was partly funded by a HART-GFZ grant. Thanks to Kate Clark and colleagues at GNS Science (Lower Hutt) and Sharyn Goldstien and Islay Marsden (Biological Sciences, University of Canterbury) for early discussion on methodology and distribution of intertidal biota at Kaikōura. Thanks also to Rongjang Wang (GFZ) for providing his *smbloc*-code for the calculation of static offset from strong-motion data and to Dick Beetham for his able assistance during fieldwork.

Competing interests

The authors declare that they have no conflict of interest

References

Adams, N. M.: Seaweeds of New Zealand: an illustrated guide, Canterbury University Press, Christchurch, New Zealand, 1994.

Bodin, P. and Klinger, T.: Coastal uplift and mortality of intertidal organisms caused by the September 1985 Mexico earthquakes, Science, 233, 1071-1073, 1986.

Carver, G.A., Jayko, A.S., Valentine, D.W., and Li, W.H.: Coastal uplift associated with the 1992 Cape Mendocino earthquake, northern California, Geology, 22, 195-198, 1994.

Castilla, J.C.: Earthquake-caused coastal uplift and its effect on rocky intertidal kelp communities, Science, 242, 440-443, 1988.

Castilla, J.C and Oliva, D.: Ecological consequences of coseismic uplift on the intertidal kelp belts of *Lessonia nigrescens* in

central Chile, Estuarine, Coas. Sh. S., 31, 45-56, 1990.

Castilla, J.C., Manríquez, P.H., and Camaño, A.: Effects of rocky shore coseismic uplift and the 2010 Chilean mega-earthquake on intertidal biomarker species, Mar. Ecol. Progr. Ser., 418, 17-23, 2010.

Cesca, S., Zhang, Y., Mouslopoulou, V., Wang, R., Saul, J., Savage, M., Heimann, S., Kufner, S.-K., Oncken, O., and Dahm, T.: Complex rupture process of the Mw 7.8, 2016, Kaikoura earthquake, New Zealand, and its aftershock sequence, Earth Planet. Sci. Lett., 478, 110-120, https://doi.org/10.1016/j.epsl.2017.08.024, 2017.

Clark, K.J., Nissen, E.K., Howarth, J.D., Hamling, I.J., Mountjoy, J.J., Ries, W.F., Jones, K., Goldstien, S., Cochran, U.A., Villamor, P., Hreinsdóttir, S., Litchfield, N.J., Mueller, C., Berryman, K.R., and Strong, D.T.: Highly variable coastal deformation in the 2016 MW7.8 Kaikōura earthquake reflects rupture complexity along a transpressional plate boundary, Earth Planet. Sci. Lett., 474, 334-344, 2017.

De Mets, C.R., Gordon, R.G., Argus, D., Stein, S., 1994. Effect of recent revisions to the geomagnetic reversal time scale on estimates of current plate motions, Geophys. Res. Lett., 21, 2191-2194, 1994.

Eberhart-Phillips, D. and Bannister, S.: 3-D imaging of Marlborough, New Zealand, subducted plate and strike-slip fault systems, Geophys. J. Intern., 182, 73-96, 2010.

Farías, M., Vargas, G., Tassara, A., Carretier, S., Baize, S., Melnick, D., and Bataille, K.: Land-level changes produced by the Mw 8.8 2010 Chilean earthquake, Science, 329, 916, 2010.

Fitzroy, R.: Proceedings of the second expedition, 1831-1836: under the command of Captain Robert Fitzroy. Volume II of the narrative of the surveying voyages of His Majesty's ships Adventure and Beagle between Years 1826 and 1836, describing their examination of the southern shores of South America, and the Beagle's circumnavigation of the globe, London, UK, 1839.

Garrison, T.: Oceanography: An Invitation to Marine Science, Seventh Edition, Thomson Learning, Brooks/Cole, 2010.

Graham, M.: "An account of some effects of the late earthquakes in Chili. Extracted from a letter to Henry Warburton, Esq V.P.G.S". Transactions of the Geological Society of London, Second Series 1, Part 2, 413-415, 1824.

Hamling, I. J. et al.: Complex multi-fault rupture during the 2016 Mw 7.8 Kaikōura earthquake, New Zealand, Science, doi:10.1126/science.aam7194, 2017.

Hay, C.H. and South, G.R.: Experimental ecology with particular reference to proposed commercial harvesting of *Durvillaea* (Phaeophyta, Durvillaeales) in New Zealand. Bot. Mar., 22, 431-436, 1979.

Jaramillo, E., Melnick, D., Baez, J.C., Montecino, H., Lagos, N.A., Acuña, E., Manzano, M., and Camus, P.A.: Calibrating coseismic coastal land-level changes during the 2014 Iquique (Mw=8.2) earthquake (northern Chile) with leveling, GPS and intertidal biota. PLoS ONE 12, e0174348, 2017.

Kaiser, A., et al.: The 2016 Kaikōura, New Zealand, Earthquake: Preliminary Seismological Report, Seismol. Res. Lett., 88, DOI: 10.1785/0220170018, 2017.

Laborel, J. and Laborel-Deguen, F.: Biological indicators of relative sea-level variations and of co-seismic displacements in the Mediterranean region, J. Coast. Res. ,10, 395-415, 1994.

Deleted: Clark, K.J., Johnson, P.N., Turnbull, I.M., and Litchfield, N.J.: The 2009 Mw 7.8 earthquake on the Puysegur subduction zone produced minimal geological effects around Dusky Sound, New Zealand, New Zeal. J. Geol. Geop., 54, 237-247, 2011.¶

Litchfield N., et al.: Surface Fault Rupture from the Mw 7.8 2016 Kaikōura Earthquake, New Zealand, and Insights into Factors Controlling Multi-Fault Ruptures, Bull. Seismol. Soc. Am., 108, 1496-1520. doi.org/10.1785/0120170300, 2018.

Marsden, I.D.: Between the tides on the Kaikoura Peninsula, Mauri Ora, 12, 69-93, 1985.

Melnick, D., Cisternas, M., Moreno, M., and Norambuena, R.: Estimating coseismic coastal uplift with an intertidal mussel: calibration for the 2010 Maule Chile earthquake (Mw = 8.8), Quatern. Sci. Rev., 42, 29-42, 2012.

Mouslopoulou, V., Begg, J.G., Nicol, A., Oncken, O., and Prior, C.: Formation of Late Quaternary paleoshorelines in Crete, Eastern Mediterranean, Earth Planet. Sci. Lett., 431, 294-307, 2015a.

Mouslopoulou, V., Nicol, A., Begg, J., Oncken, O., and Moreno, M.: Clusters of mega-earthquakes on upper plate faults control the Eastern Mediterranean hazard, Geophys. Res. Lett., 42, 10,282–10,289, doi:10.1002/2015GL066371, 2015b.

Mouslopoulou, V., Saltogianni, V., Nicol, A., Oncken, O., Begg, J., Babeyko, A., Cesca, S., and Moreno, M.: Breaking a subduction-termination from top-to-bottom: the 2016 Kaikōura earthquake, Earth Planet. Sci. Lett., 506, 221-230, https://doi.org/10.1016/j.epsl.2018.10.020, 2019.

Nelson, W.: New Zealand Seaweeds; an Illustrated Guide, Te Papa Press, Wellington, New Zealand, 2013.

Nicol A., Khajavi N., Pettinga J., Fenton C., Stahl T., Bannister S., Pedley KL., Hyland-Brook N., Bushell T., and Hamling I.: Preliminary geometry, slip and kinematics of fault ruptures during the 2016 MW 7.8 Kaikōura Earthquake in the North Canterbury region of New Zealand, Bull. Seismol. Soc. Am., 108, 1521-1539, 2018.

Ortlieb, L., Barrientos, S., and Guzmán, N.: Coseismic coastal uplift and coralline algae record in Northern Chile: the 1995 Antofagasta earthquake case, Quatern. Sci. Rev., 15, 949-960, 1996.

Pirazzoli, P., Thommeret, J., Thommeret, Y., Laborel, J., and Montaggioni, L.: Crustal block movements from Holocene shorelines: Crete and Antikythira (Greece), Tectonophysics, 86, 27-43, 1982.

Pirazzoli, P.A., Delibrias, G., Kawana, T., and Yamaguchi, T.: The use of barnacles to measure and date relative sea-level changes in the Ryukyu Islands, Japan. Palaeogeogr., Palaeoecl., 49, 161-174, 1985.

Plafker, G.: Tectonic deformation associated with the 1964 Alaska earthquake, Science, 148, 1675-1687, 1965.

Plafker, G. and Ward, S.N.: Backarc thrust faulting and tectonic iplift along the Caribbean sea coast during the April 22, 1991 Costa Rica earthquake, Tectonics, 11, 709-718, 1992.

Pondard, N. and Barnes, P.M.: Structure and paleoearthquake records of active submarine faults, Cook Strait, New Zealand: Implications for fault interactions, stress loading, and seismic hazard, J. Geophys. Res., 115, B12320, doi:12310.11029/12010JB007781, 2010.

Power, W., Clark, K., King, D.N., Borrero, J., Howarth, J., Lane, E.M., Goring, D., Goff, J., Chague-Goff, C., Williams, J., Reid, C., Whittaker, C., Mueller, C., Williams, S., Hughes, M., Hoyle, J., Bind, J., Strong, D.T., Litchfield, N., and Benson, A.: Tsunami runup and tide-gauge observations from the 14 November 2016 M7.8 Kaikōura earthquake, New Zealand, Pure Appl. Geophys., 174, 2457-2473, 2017.

Ramirez-Herrera, M.-T. and Orozco, J.J.Z.: Coastal uplift and mortality of coralline algae caused by a 6.3Mw earthquake, Oaxaca, Mexico J. Coast. Res., 18, 75-81, 2002.

Schurr, B., et al.: The 2007 M7. 7 Tocopilla northern Chile earthquake sequence: Implications for along-strike and downdip rupture segmentation and megathrust frictional behaviour, J. Geophys. Res., Solid Earth, 117(B5), 2012.

Stiros, S.C., Arnold, M., Pirazzoli, P.A., Laborel, J., Laborel, F., and Papageorgiou, S.: Historical coseismic uplift on Euboea Island, Greece, Earth Planet. Sci. Lett., 108, 109-117, 1992.

Vargas, G., Farías, M., Carretier, S., Tassara, A., Baize, S., and Melnick, D.: Coastal uplift and tsunami effects associated to the 2010 Mw8.8 Maule earthquake in Central Chile, Andean Geol., 38, 219-238, 2011.

Wallace, L.M., Barnes, P., Beavan, R.J., Van Dissen, R.J., Litchfield, N.J., Mountjoy, J., Langridge, R.M., Lamarche, G., and Pondard, N.: The kinematics of a transition from subduction to strike-slip: an example from the central New Zealand plate boundary, J. Geophys. Res., 117, B02405, 2012.

Wang, R., Schurr, B., Milkereit, C., Shao, Z., and Jin, M.: An improved automatic scheme for empirical baseline correction of digital strong-motion records, Bull. Seismol. Soc.Am., 101, 2029-2044, 2011

Wesson, R.L.: Darwin's First Theory, Pegasus Books, New York, 2017

Wesson, R.L., Melnick, D., Cisternas, M., Moreno, M., and Ely, L.L.: Vertical deformation through a complete seismic cycle at Isla Santa Maria, Chile, Nat. Geosci., 8, 547-551, 2015.

Figure and table captions

Figure 1: (a) Inset map of New Zealand illustrating the main tectonic features of the Hikurangi subduction margin, the location of the Marlborough Fault System (MFS) and the epicentre of the 2016 M_w 7.8 Kaikōura Earthquake. Blue box near the Kaikōura Earthquake epicentre indicates the study area. (b) Map showing the study localities from which *Durvillaea* and *Carpophyllum* holdfast measurements were recorded using RTK GNSS and tape-measure, the position of State Highway One (SH1) from which LiDAR data points were derived (see yellow line), the location of Kaikōura Tide Gauge and the KIKS strong ground motion station. The Hundalee Fault is also located. Background image supplied by Land Information New Zealand.

Figure 2: Field photographs of the intertidal zone and biota near Kaikōura (taken after the earthquake). (a) Healthy *Durvillaea* (mostly *D. willana*) (D) and *Carpophyllum* (C) photographed at low-tide. (b) uplifted bedrock north of Paia Point showing living *Carpophyllum* (C) and dead *Carpophyllum* holdfast stumps (CH). Note also the living pink coralline algae at the waterline and bleached morbid coralline algae (arrows) and bright green *Ulva*. (c) uplifted intertidal zone near the Kaikōura tide gauge, showing distinctive line of *Carpophyllum* holdfasts (CH) and dispersed *Durvillaea* holdfasts (DH). (d) uplifted intertidal zone near Paia Point. One of the authors (J.B.) measures the elevation of *Durvillaea* holdfasts (DH) and *Carpophyllum* holdfasts (CH) using RTK GNSS survey equipment. Note distinctive white zone of dead coralline algae.

Deleted: with

Deleted: illustrated

Formatted: Font: Italic

Figure 3: Schematic diagram illustrating uplift and stranding of holdfasts at the Kaikōura Tide Gauge. It also illustrates schematically the method for calculating uplift from the upper limit of holdfasts ($X_{C/D/G}$; Eq. 1) using Mean Low-Water Spring (MLWS) values within the tide-gauge data. MLWN = Mean Low-Water Neap, MHWN = Mean High-Water Neap, MHWS = Mean High-Water Spring, H_{TG} = tide height as measured in tide gauge, U_{TG} = uplift as measured by tide gauge offset data pre- and post-deformation, OM = observed measurement (holdfast), X = offset of holdfasts from MLWS. Inset: Results for X as calculated for kelp at the Kaikoura Tide Gauge. Mean values are shown by a solid-circle while tails represent maxima and minima values. See Sect. 3.2.1 for details.

Figure 4: Schematic diagram illustrating uplift and stranding of holdfasts used to calculate offset of holdfasts ($X_{NIWA/LINZ}$) from Mean Low-Water Spring (MLWS) independent from tide gauge data. MLWN = Mean Low-Water Neap. Here MLWS is determined from LINZ and NIWA predictive charts, and the position of holdfasts with respect to MLWS and MLWN is determined from local knowledge of kelp distribution (Goldstien pers. comm. 2017).

Figure 5: Uplift at the Kaikoura Tide Gauge calculated from the upper living-positions of various kelp holdfasts and exposure sites plotted against the offset recorded, at the same locality, using the tide-gauge and differential LiDAR. Holdfast data are presented as *mean* and *standard deviation* while the tide-gauge and LiDAR data are presented as *mean* only. Black numbers beside the datapoints indicate the mean values while 'n' values at the top represent the number of measurements per category.

Figure 6: (a) Tectonic uplift in metres measured at the Kaikōura Tide Gauge, Kaikōura Harbour, Paia Point and Omihi Point from biological data processed using the tide-gauge correction, and NIWA and LINZ predictive tide-chart correction methods (see Sect. 3.2). These values are compared to uplift recorded by the Tide Gauge and differential LiDAR (where available). (b) Percentage of uplift-deviation of the biological methods with respect to the LiDAR measurements. Horizontal axis not to scale.

Figure 7: Locality, digital elevation imagery and differential LiDAR data for Paia Point (see Fig. 1 for location). (a) Aerial photo from Google Earth imagery of Paia Point, State Highway-1 and uplift collection points. Blue line = portion of SH1 from which differential LiDAR uplift calculated, red circles: RTK-GPS collected kelp data-points, yellow circles: tape-measure collected kelp data-points. (b) Digital Elevation Model developed from post-earthquake LiDAR data. Blue line and colour-coded circles as per (a). (c) Plot of uplift of points at 1 m intervals along the blue line on SH1 in (a) and (b) derived from differential LiDAR.

Deleted: offset
Deleted: from
Deleted: of
Deleted: measured
Deleted: at
Deleted: by
Deleted: T
Deleted: G
Deleted: T
Deleted: G
Formatted: English (New Zealand)

Figure 8: Cross plots of data collection and processing methods. (a) RTK and tape-measure uplift data processed using the tide-gauge correction method. (b) RTK uplift data, processed using the tide-gauge correction method, plotted against differential LiDAR uplift data. (c) Tape-measure uplift data, processed using tide-gauge correction method, plotted against differential LiDAR uplift data. (d) RTK uplift data, processed using the tide-gauge correction method, plotted against the NIWA Forecaster tide chart correction method.

Table 1: Calculation of uplift at the Kaikōura Tide Gauge (KAIT) using tide-gauge readings for high and low spring-tides and high and low neap-tides (see Sect. 3.1).

Table 2: Absolute uplift values calculated from the Kaikōura Tide Gauge data using methods B-E. Method B: Comparison of average high-tide and low-tide readings from several tidal cycles (3-day period) before and after the earthquake; Method C: Aligning pre-earthquake tidal data with post-earthquake data and incrementally adjusting them until a best fit; Method D: comparing the average water-elevation from a pre-earthquake month to the same month's data after the earthquake (December 2015 against December 2016); Method E: Calculating the difference in average waterline elevations for an extended period (44 days) before and after the earthquake (Nov 14th to Dec 27th). As Method A here we refer the methodology established in Sect. 3.1 and presented in Table 1.

Table 3: Results for calculation of the upper living position $X_{C/D/G}$ relative to MLWS for holdfasts at the Kaikōura Tide Gauge. Note, that only holdfasts of *Carpophyllum* and *Durvillaea* in sheltered locations were used to calculate this elevation.

Table 4: Comparison of uplift results for data collected by RTK and tape-measure at the tide-gauge and including a comparison of kelp types in both sheltered and exposed locations. Results are presented by holdfast species and exposure ranking, independently of the collection site.

Table 5: Comparison of mean uplift values derived using RTK for the various methodologies (e.g., tide-gauge calibration method, NIWA Forecaster method, LINZ Tide Chart method). As the source data remain the identical for each method, the standard deviation reflects error derived from the RTK measurements. Data is presented by site at each location; where a site was collected using both *Carpophyllum* and *Durvillaea*, the holdfast type is recorded as "mixed".

Table 6: Uplift calculated from differential LiDAR and strong-motion uplift estimated from the KIKS station.

Deleted:
Deleted: -depth
Deleted: depth
Deleted: ,
Deleted: T
Deleted: G

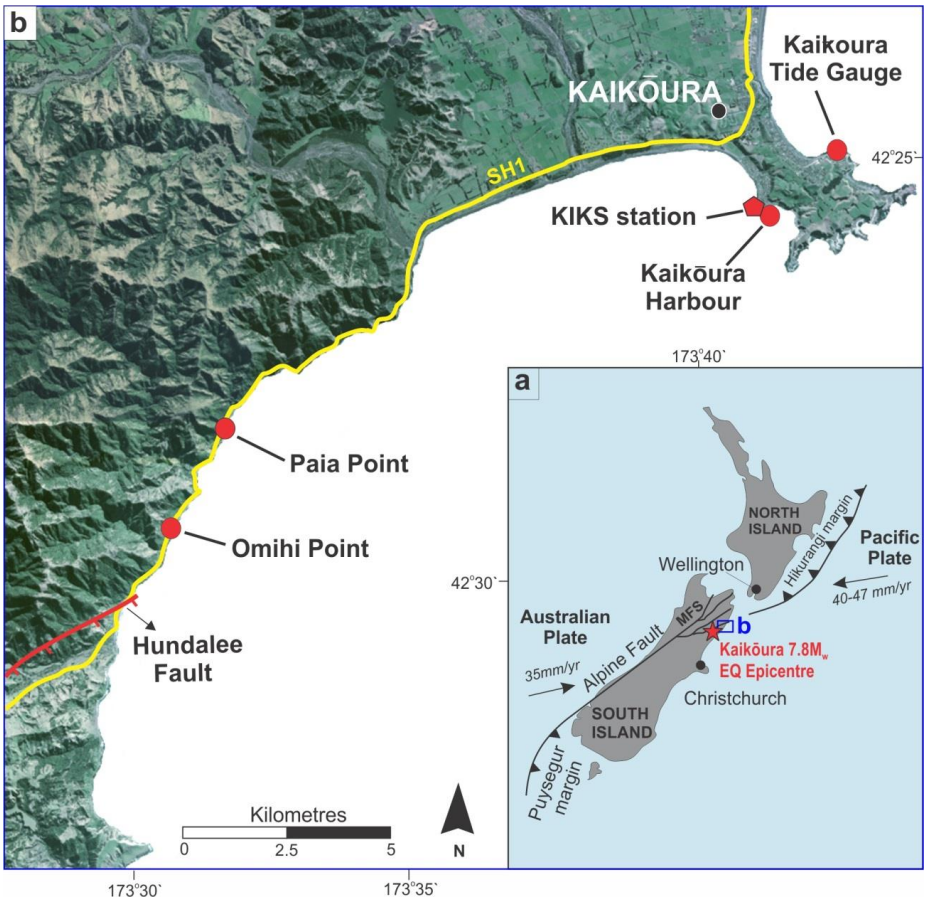
b
KAIKŌURA
Kaikoura
Tide Gauge
SH1
KIKS station
Kaikōura
Harbour
42°25`
173°40`
Paia Point
Omihi Point
Hundalee
Fault
42°30`
a
NORTH
ISLAND
Wellington
Hikurangi margin
Pacific
Plate
40-47 mm/yr
Australian
Plate
MFS
b
Kaikōura 7.8Mw
EQ Epicentre
35mm/yr
Alpine Fault
Christchurch
SOUTH
ISLAND
Puysegur
margin
Kilometres
0
2.5
5
N
173°30`
173°35`

Figure 1

Figure 2

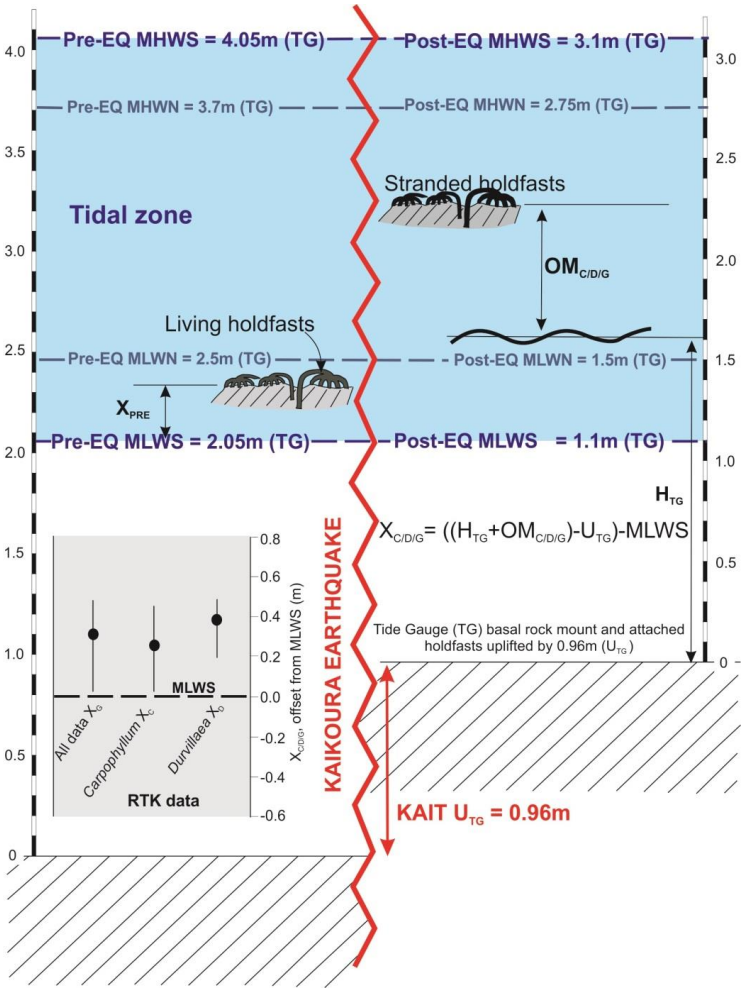

Deleted: <object>

Figure 3

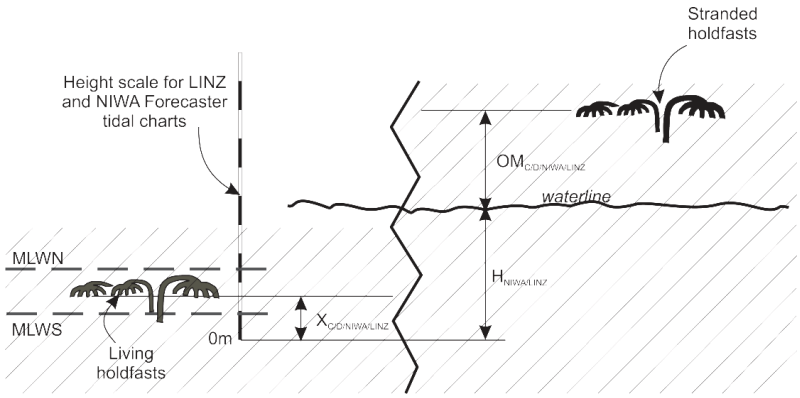

925

Figure 4

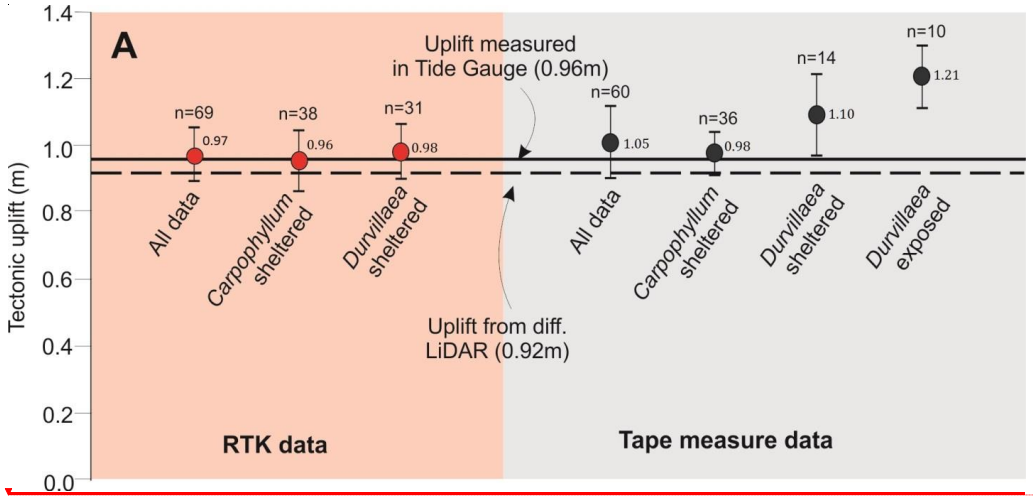

930

Figure 5

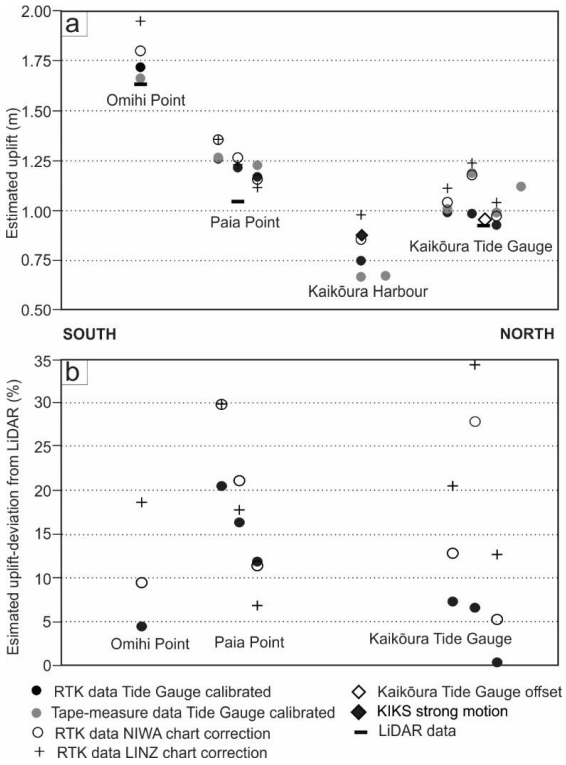
a
Estimated uplift (m)
2.00
1.75
1.50
1.25
1.00
0.75
0.50
Omihi Point
Paia Point
Kaikōura Harbour
Kaikōura Tide Gauge
SOUTH
NORTH
b
Esimated uplift-deviation from LiDAR (%)
35
30
25
20
15
10
5
0
Omihi Point
Paia Point
Kaikōura Tide Gauge
RTK data Tide Gauge calibrated
Tape-measure data Tide Gauge calibrated
RTK data NIWA chart correction
RTK data LINZ chart correction
Kaikōura Tide Gauge offset
KIKS strong motion
LiDAR data

Figure 6

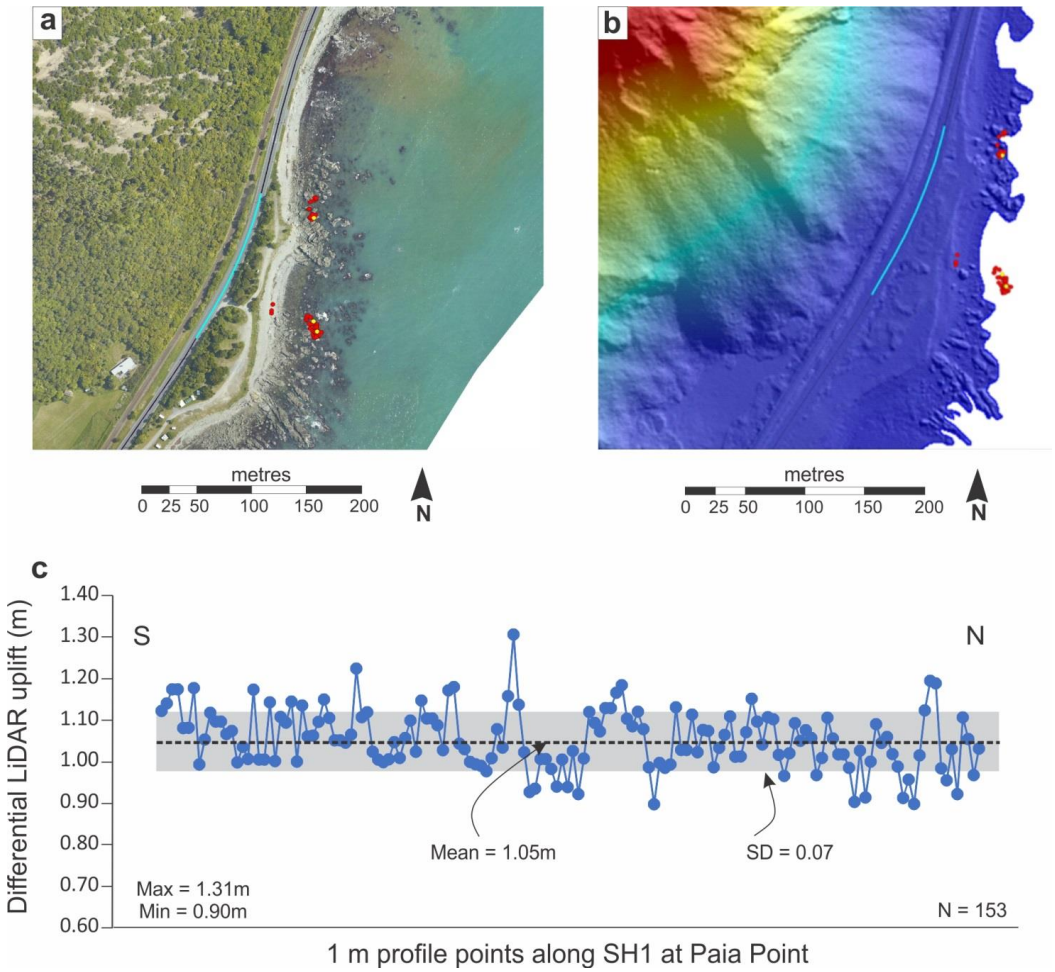
a
b
metres
0 25 50 100 150 200
N
metres
0 25 50 100 150 200
N
c
Differential LiDAR uplift (m)
1.40
1.30
1.20
1.10
1.00
0.90
0.80
0.70
0.60
S
N
Mean = 1.05m
SD = 0.07
Max = 1.31m
Min = 0.90m
N = 153
1 m profile points along SH1 at Paia Point

Figure 7

950

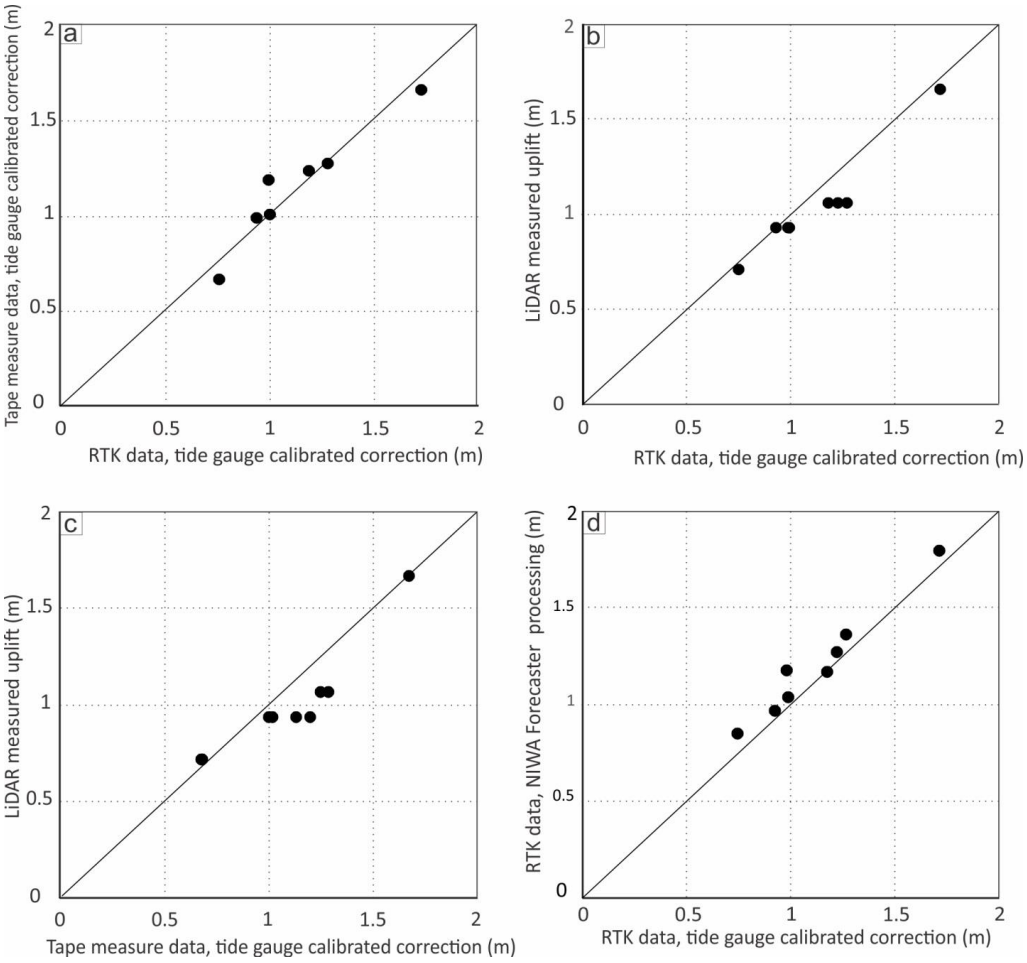

955

Figure 8

960

	Spring tide		Neap tide		Uplift	
	Pre-EQ	Post-EQ	Pre-EQ	Post-EQ	Spring diff	Neap diff
High tide	4.05m	3.1m	3.7m	2.75m	0.95m	0.95m
Low tide	2.05m	1.1m	2.5m	1.5m	0.95m	1m
Range	2m	2m	1.2m	1.25m	**Mean diff**	**0.96m**

Table 1

Method	Data points	Mean uplift (m)
A		0.96
B	6	0.95
C	17568	0.98
D	44640	0.96
E	17932	0.97
	Overall mean uplift U_{TG}	**0.96**
	Standard deviation	**0.02**

Table 2

	Mean	SD	Median	Max	Min
All holdfasts X_G	0.31m	0.10m	0.32m	0.50m	0.01m
***Carpophyllum* X_C**	0.26m	0.09m	0.26m	0.43m	0.01m
***Durvillaea* X_D**	0.38m	0.07m	0.39m	0.50m	0.19m

Table 3

	Mean (m)	SD (m)	Min (m)	Max (m)
RTK data				
All data	0.97	0.08	0.71	1.13
Carpophyllum sheltered	0.96	0.09	0.71	1.13
Durvillaea sheltered	0.98	0.07	0.78	1.09
Tape measure data				
All data	1.05	0.11	0.87	1.35
Carpophyllum sheltered	0.98	0.06	0.87	1.13
Carpophyllum exposed	1.06	0.07	0.92	1.22
Durvillaea sheltered	1.10	0.13	0.91	1.35
Durvillaea exposed	1.21	0.09	1.07	1.35

Table 4

Site	Holdfast type	Tide Gauge Mean (m)	NIWA Forecaster Mean (m)	LINZ Tide Charts Mean (m)	SD* (m)
RTK					
Tide Gauge 1	*Carpophyllum*	0.99	1.04	1.11	0.06
Tide Gauge 2	*Carpophyllum*	0.92	0.97	1.04	0.10
Tide Gauge 3	*Durvillaea*	0.98	1.18	1.24	0.07
Paia Point 1	*Carpophyllum*	1.27	1.27	1.24	0.11
Paia Point 2	*Durvillaea*	1.22	1.36	1.36	0.18
Paia Point 3	Mixed	1.18	1.17	1.12	0.16
Omihi Point 1	*Carpophyllum*	1.71	1.80	1.95	0.13
Kaikōura Hbr	*Carpophyllum*	0.74	0.85	0.98	0.12
Tape Measure					
Tide Gauge 1	*Carpophyllum*	1.00			0.07
Tide Gauge 2	*Carpophyllum*	1.12			0.11
Tide Gauge 3	*Durvillaea*	1.19			0.08
Tide Gauge 4	Mixed	0.99			0.06
Paia Point 1	Mixed	1.27			0.09
Paia Point 2	Mixed	1.23			0.09
Omihi Point 1	Mixed	1.66			0.17
Kaikōura Hbr	*Carpophyllum*	0.66			0.10
Kaikōura Hbr	*Carpophyllum*	0.67			0.06

Table 5

	Mean (m)	Median (m)	SD (m)	Max (m)	Min (m)
Differential LiDAR					
Tide Gauge	0.92	0.91	0.06	1.13	0.77
Paia Point	1.05	1.05	0.07	1.31	0.90
Omihi Point	1.64	1.64	0.04	1.74	1.53
KIKS Strong motion					
Kaikōura Harbour	0.87	0.06			

Table 6